Article

Identifying the Spectral Signatures of Invasive and Native Plant Species in Two Protected Areas of Pakistan through Field Spectroscopy

Iram M. Iqbal [1,2,*] ![ORCID], **Heiko Balzter** [2,3] ![ORCID], **Firdaus-e-Bareen** [1] **and Asad Shabbir** [1,4] ![ORCID]

1   Ecology and Evolution Lab, Institute of Botany, University of the Punjab, Quaid-e-Azam Campus, Lahore 54590, Pakistan; firdaus.botany@pu.edu.pk (F.-e.-B.); asad.iags@pu.edu.pk (A.S.)
2   Centre for Landscape and Climate Research, School of Geography, Geology and Environment, University of Leicester, Leicester LE1 7RH, UK; hb91@le.ac.uk
3   National Centre for Earth Observation, Leicester LE1 7RH, UK
4   School of Life and Environmental Sciences, University of Sydney, Camden 2570, Australia
*   Correspondence: iram.phd.botany@pu.edu.pk

Abstract: Globally, biological invasions are considered as one of the major contributing factors for the loss of indigenous biological diversity. Hyperspectral remote sensing plays an important role in the detection and mapping of invasive plant species. The main objective of this study was to discriminate invasive plant species from adjacent native species using a ground-based hyperspectral sensor in two protected areas, Lehri Reserve Forest and Jindi Reserve Forest in Punjab, Pakistan. Field spectral measurements were collected using an ASD FieldSpec handheld2™ spectroradiometer (325–1075 nm) and the discrimination between native and invasive plant species was evaluated statistically using hyperspectral indices as well as leaf wavelength spectra. Finally, spectral separability was calculated using Jeffries Matusita distance index, based on selected wavebands. The results reveal that there were statistically significant differences ($p < 0.05$) between the different spectral indices of most of the plant species in the forests. However, the red-edge parameters showed the highest potential ($p < 0.001$) to discriminate different plant species. With leaf spectral signatures, the mean reflectance between all plant species was significantly different ($p < 0.05$) at 562 (75%) wavelength bands. Among pairwise comparisons, invasive *Leucaena leucocephala* showed the best discriminating ability, with *Dodonaea viscosa* having 505 significant wavebands showing variations between them. Jeffries Matusita distance analysis revealed that band combinations of the red-edge region (725, 726 nm) showed the best spectral separability (85%) for all species. Our findings suggest that it is possible to identify and discriminate invasive species through field spectroscopy for their future monitoring and management. However, the upscaling of hyperspectral measurements to airborne and satellite sensors can provide a reliable estimation of invasion through mapping inside the protected areas and can help to conserve biodiversity and environmental ecosystems in the future.

Keywords: discrimination; hyperspectral data; *Lantana camara*; *Prosopis juliflora*; spectroradiometer; invasive species management

1. Introduction

Protected areas provide a refuge for native species and help to protect biodiversity by acting as natural filters, especially against biological invasions [1]. However, biological invasions are still the second-largest global threat to biodiversity after habitat loss [2,3]. Invasive plant species negatively affect the native species through direct competition for resources, changing ecosystem processes or through allelopathy [4]. The negative impacts of invasive species have been widely studied by scientists in recent years and a range of management strategies have been suggested [5,6]. To help land managers, one of the earliest steps in planning effective management is to collect accurate information on the spatial

distribution of invasive species [7]. Traditional methods of mapping the distribution of invasive species generally require intensive fieldwork that involves visual observation and identification of plant species along with their richness and diversity [8,9]. The limitations of such field assessment methods include high cost, excessive time consumption, site accessibility constraints, reliance on highly subjective methods, and visual calculation errors that may yield inaccurate distribution assessment, ultimately leading to poor management strategies for invasive species [10]. Therefore, it is critical to use advanced and more reliable techniques to assess and monitor the invasions, and develop effective management programs [11].

Remote sensing plays an important role in the early detection and quantification of alien invasive vegetation cover [12,13] and is now recognized as an important tool for ecologists, agriculturalists, and land managers for understanding and managing many environmental issues [14–16]. The remote sensing of vegetation involves the use of different imaging and non-imaging sensors to obtain spectral measurements of plant species [17] by a range of airborne and space-borne sensors (multispectral or hyperspectral) with coarse to high spatial resolutions [18,19].

The spectral diversity of plant species represents the variations existing in spectral patterns that are detected by optical remote sensing [20]. Studies have shown that each plant species, whether native or invasive, has unique spectral reflectance due to dissimilar physical and biochemical characteristics that ultimately help to facilitate species-level identification [21,22]. Therefore, it is often possible to differentiate plant species using their spectral diversity [23,24]. Thus, invasive plant species may be separated from native species due to their distinct reflectance, biochemical and structural properties [25,26].

Multispectral imaging sensors are important in detecting the invasion of forest ecosystems or larger areas [27–29]. However, hyperspectral non-imaging sensors (e.g., handheld spectroradiometers) are a more reliable source for discriminating small variations between species and other biochemical properties [7,30]. Narrow bands of hyperspectral sensors can enable the finer discrimination of plants' physiological processes by measuring species level changes, leading to improved detection and mapping of invasive species [25,31]. Multispectral remote sensing is somewhat challenging in discriminating and mapping plant species due to its low spectral and spatial resolution as well as the spectral overlapping that may result in less accuracy [32]. The contiguous narrow bands of hyperspectral data have led to the successful spectral separation of native and invasive species, either by hyperspectral satellite images [13,29,33,34] or by field-based instruments [7,35]. However, the high cost of hyperspectral satellite data somehow limits its usage at a small academic level, especially in developing countries.

The discrimination and detection of invasive species using multi or hyperspectral remote sensing is an important step to take before developing any management strategies. Several studies have shown the importance of hyperspectral field spectroscopy for early plant detection and discrimination using different separability approaches, statistical techniques and feature selection methods. Cochrane [36] studied the spectral differences between different plant species of tropical forests using hyperspectral ASD spectroradiometer (350–1050 nm) under laboratory conditions. Similarly, tropical mangrove species were identified using statistical techniques of ANOVA as well as Jeffries Matusita (JM) separability index in VNIR (Visible and Near Infrared) and SWIR (Short Wavelength Infrared) range (350–2500 nm) under a laboratory environment [37]. Ullah and colleagues [38] also revealed significant differences between tropical plant species in the Netherlands using mid-wave (2.5–6 μm) and thermal (8–14 μm) measurements of the leaf spectra. In addition to lab spectral measurements, ground-based hyperspectral remote sensing was also extensively used to distinguish different plant species in the field [39]. Schmidt and Skidmore [40] discriminated different vegetation types in the coastal saltmarsh of the Netherlands with the help of GER 3700 spectrometer (325–2509 nm) using ANOVA and JM distance analysis. *Cyperus papyrus* L. was also successfully discriminated from its co-existent wetland species using ANOVA, CART and JM distance analysis in St. Lucia

Wetlands Park in South Africa [41]. Recently, Aneece and Epstein [42] identified six invasive plant species (*Galium verum* L., *Ailanthus altissima* (Mill.) Swingle, *Celastrus orbiculatus* Thunb., *Rhamnus davurica* Pall., *Carduus acanthoides* L., and *Cirsium arvense* (L.) Scop.) in crop fields in Northern Virginia using ANOVA and SVM analysis and revealed that the 350–399, 500–549, 700–749, and 900–949 nm regions were the most significant regions for discriminating different species in the field. Taylor et al. [43] also used a spectroradiometer (350–2500 nm) to successfully discriminate invasive rhododendron from other co-existing species using Kruskal–Wallis and logistic regression model. These studies are based on the variations between spectral signatures of different plant species. However, the potential of hyperspectral indices, as well as red-edge parameters (REPs), has also previously been studied for discriminating between the spectral diversity of plant species [44–46] Cho et al. [47] evaluated the potential of spectral indices by using leaf and canopy spectra of six different species and found REP, NDVI, and PRI as good indices for the spectral identification of plant species. Similarly, invasive *Acacia longifolia* (Andrews) Willd. was able to be discriminated using field VNIR-SWIR spectra as well as narrowband hyperspectral indices in a Mediterranean dune ecosystem in Portugal [48]. All these studies highlight the potential role of field spectroscopy in discriminating invasive species.

The application of remote sensing in invasive species' mapping and monitoring is currently not very advanced in Pakistan. In an attempt to classify the vegetation of metropolitan city of Karachi, Pakistan, Shehzad et al. [49] classified invasive *Prosopis juliflora* on high-resolution Worldview-2 imagery using object-based classification in a relatively small area of northwest Karachi, Pakistan. Recently, Kazmi et al. [50] used GeoEye multispectral and Hyperion EO-1 hyperspectral data to map *P. juliflora* with 93 and 99% accuracy in urban and semiurban areas of Karachi. However, to the best of our knowledge, no studies reported on the discrimination of invasive species from other co-existing native species of protected areas using ground-based hyperspectral data in Pakistan.

Therefore, this is the first study of its kind with the aims:

1. To explore the potential of hyperspectral data to discriminate invasive and native plant species using hyperspectral indices as well as wavelength spectra in the Lehri and Jindi Reserve forests
2. To identify diagnostic wavelength regions for better identification and separability of plant species.
3. To determine the best band combinations for spectral separability of plant species of different geographic origins using the Jeffries Matusita distance.

2. Materials and Methods

2.1. Site Description

The study area covers two scrub forests of the district Jhelum of the Punjab province, Pakistan. The Lehri Reserve Forest (33.15° N, 73.59° E; 463 m asl) covers an area of 4843.3 hectares while Jindi Reserve Forest (33.06° N, 73.47° E; 407 m asl) spans over 2163.1 hectares (Figure 1). Collectively, both forests were named as Lehri Nature Park in 1987 for the protection and conservation of natural flora and fauna. Both forests have semievergreen scrub vegetation with overall subhumid to dry climate. The temperature ranges from 8 °C to 42 °C, January being the coldest and June the hottest month of the year. Average annual rainfall is about 850 mm. The vegetation is mainly subtropical dry evergreen open scrub, dominated by *Dodonaea viscosa* (L.) Jacq., *Acacia modesta* Wall., *Olea ferruginea* Wall. ex Aitch., *Ziziphus nummularia* (Burm.f.) Wight and Arn., *Prosopis juliflora* L. and *Heteropogon contortus* (L.) P.Beauv. ex Roem. and Schult [51] (Figure 2).

The Lehri Nature Park is located in the Potohar region in the east of the salt range with an elevation ranging from 250 m to 1025 m [52]. The northern region of Lehri RF has a water reservoir, Mangla, while its east and west regions share boundaries with the Mangla Cantonment area and Lehri Town, respectively. Both forests share a common boundary in the south of Lehri RF. However, the southern boundary of Jindi RF touches the Grand

Trunk Road linking two provincial capital cities, Lahore and Peshawar. Topographically, the area consists of rugged and steep mountains having low height with dense vegetation cover, while mountain rocks are majorly comprised of sandstone and limestone (Figure 2).
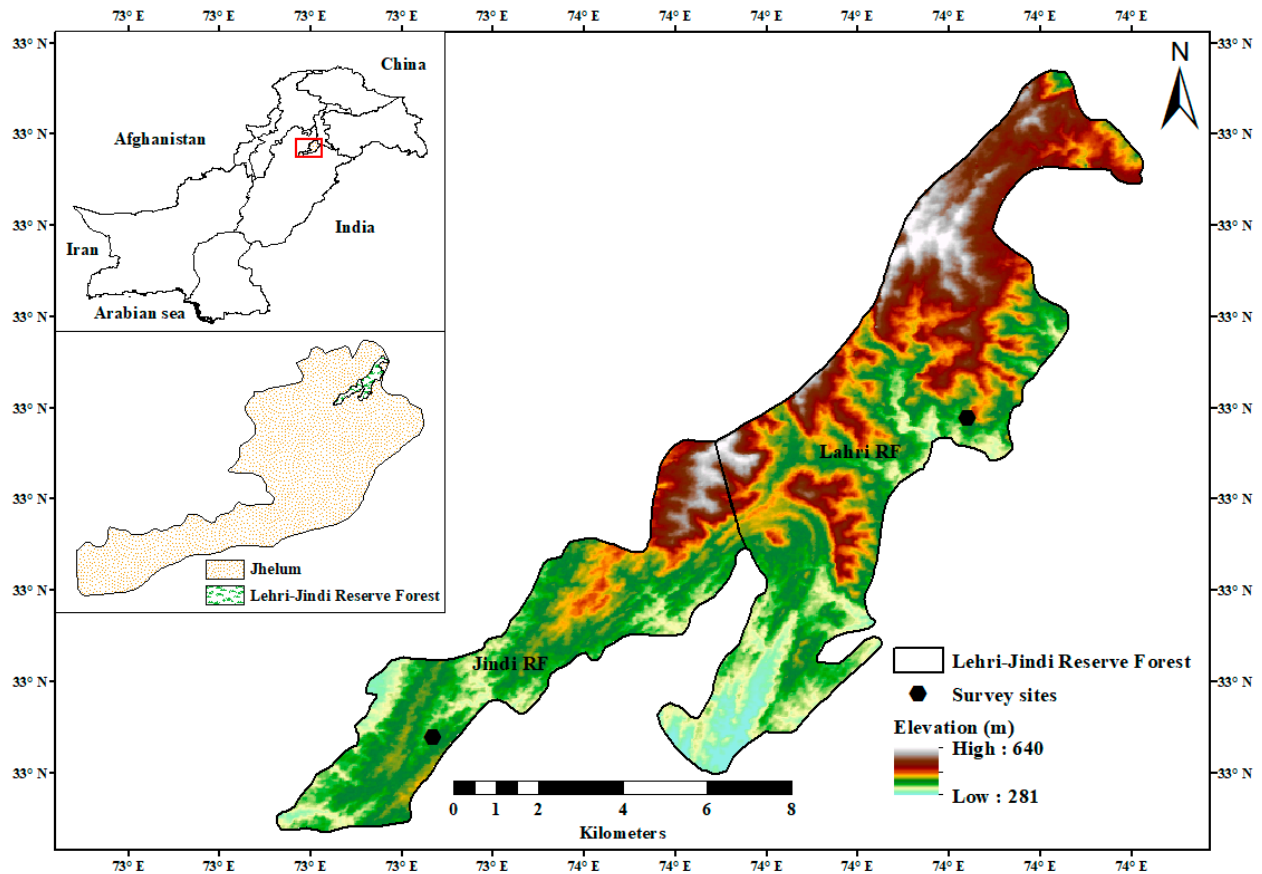
Figure 1. Map of the study area located in the north of the district Jhelum in the Punjab Province, Pakistan.

(**a**)   (**b**)

Figure 2. Topography of the study area showing dry scrub forest vegetation with stands of *A. modesta* and *L. camara* (**a**) and *D. viscosa* (**b**) in the district Jhelum, Punjab, Pakistan.

2.2. Field Data Collection

2.2.1. Site Selection and Target Species

Field surveys were conducted at the end of the summer season in October 2018 and 2019 to record the spectral signatures of plant species. Lehri–Jindi Reserve forests are scrub forests with dense vegetation, making it difficult to access the remote regions inside the forests.

Therefore, two accessible sites (one in each reserve forest) were selected for the collection of field data (Figure 1) and were considered as representative sites for the current study.

The current study aimed to discriminate invasive plant species from other co-occurring species in the field. Therefore, different plant species associated with major invasive species of the forests were selected through field observation techniques and based on the visual abundance assessment. Three main categories of plant species (native, invasive, and ornamental) were designated and prioritized for spectral sampling. Plants that were introduced/cultivated but did not result in unpleasant consequences for the local ecosystems were identified as ornamental. Details of each species are given in Table 1.

Table 1. Characteristics of plant species selected for the current study.

Category	Plant Species	Common Name	Family	Habit
Native	*Justicia adhatoda* L.	Malabar nut	Acanthaceae	shrub
	Acacia modesta Wall.	Hook thorn tree	Fabaceae	tree
	Dodonaea viscosa (L.) Jacq.	Switch sorrel	Sapindaceae	shrub
Invasive	*Parthenium hysterophorus* L.	Carrot grass	Asteraceae	herb
	Prosopis juliflora (Sw.) DC.	Mesquite	Fabaceae	tree
	Leucaena leucocephala (Lam.) de Wit	White lead tree	Fabaceae	tree
	Lantana camara L.	Red sage	Verbenaceae	shrub
Ornamental	*Eucalyptus camaldulensis* Dehnh.	River red gum	Myrtaceae	tree
	Pongamia pinnata (L.) Pierre	Pogam oil tree	Fabaceae	tree
	Tecoma stans (L.) Juss. ex Kunth	Yellow trumpet bush	Bignoniaceae	shrub
	Callistemon viminalis (Sol. ex Gaertn.) G.Don	Bottle brush	Myrtaceae	tree

2.2.2. Spectral Sampling

Surface reflectance spectra of leaves were collected using a portable ASD FieldSpec Handheld 2™ Spectroradiometer. This spectroradiometer is a type of non-imaging sensor that measures electromagnetic radiation in the range from 325 nm to 1075 nm at a nominal spectral resolution of less than 3 nm covering 751 spectral bands. A white reference panel (99% R value), made of spectralon material, was used to calibrate the spectroradiometer, before taking the actual readings (Figure 3a). The calibration was performed regularly (after every 20 readings) to maintain homogenous spectral readings as well as to offset any changes in solar illumination or weather [7,53].

Multiple readings were taken by placing the spectroradiometer at 2 to 5 inches above the leaf adaxial surface (upper), depending upon the size of the leaf in different plant species (Figure 3b). Each leaf spectrum was sampled 3 times to reduce handling errors. Therefore, three leaf spectra per plant were taken from each plant species. The internal spectrum count was fixed at 10 scans per reading and the integration time of the spectrum was 8.5 ms. All measurements were taken under sunny conditions between 9:00 a.m. and 3:00 p.m. local time on 8 October 2018, and 30 October 2019. A handheld GPS device (model ETREX 20, GARMIN) was also used to record the coordinates and altitudes of all plant species, along with spectral sampling. The local weather conditions were also noted.

2.3. Processing of Field Spectra

The spectral data files (.asd format) acquired with the spectroradiometer were imported using the software HH2 Sync. This software only helps to store data on hardware. However, another ASD software application, View Spec Pro, was installed for displaying the spectral reflectance curves and to visualize vegetation spectral properties of plants. ASD data files were then exported into Microsoft Excel to extract all reflectance values at each wavelength (751 hyperspectral bands from 325 nm to 1075 nm wavelength) acquired from the in-situ instrument. Descriptive statistics, i.e., mean, and standard error, were calculated for whole spectral curves of each plant species (Table S1), and mean reflectance curves were converted to graphs for direct visualization and comparison.
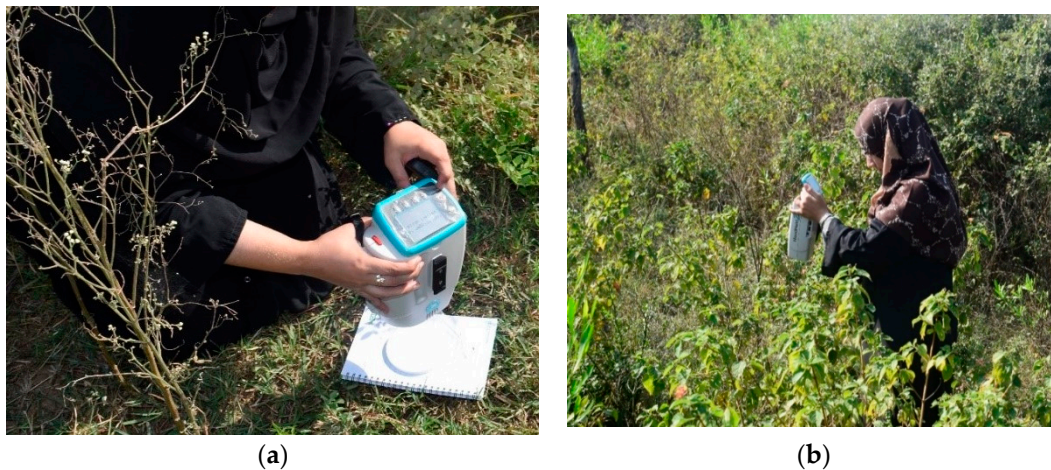
| (**a**) | (**b**) |

Figure 3. Data collection using the field spectroradiometer. Calibration using white reference panel avoiding shade (**a**); and taking the spectral reflectance of *Lantana camara* in the field (**b**).

2.4. Calculation of Spectral Indices

Different narrow-banded hyperspectral vegetation indices were derived from spectral measurements to allow species-level identification of plants [45,54]. These indices were based on the variations in chlorophyll absorption, greenness, water absorption, and other pigments at different wavelengths in the electromagnetic spectrum. The equations and significance of indices are shown in Table 2.

Table 2. Summary of different hyperspectral indices derived in the current study.

Narrowband Spectral Indices	Equations	Significance	Reference
Narrow-banded NDVI = Normalised difference vegetation index	$(R830–R670)/(R830 + R670)$	Canopy greenness, leaf area index, fraction of photosynthetically active radiation	[55]
GMI = Gitelson and Merzylak index	$(R750)/(R700)$	Chlorophyll content	[56]
PRI= Photochemical reflectance index	$(R531 − R570)/(R531 + R570)$	Conversion of xanthophylls-cycle pigments, photosynthetic light use efficiency, LAI	[57]
GI = Greenness index	$R554/R677$	Indicator of prolonged vegetation stress due to changes in canopy structure	[58]
LCI = Leaf Chlorophyll Index	$(R850–R710)/(R850 + R680)$	Total chlorophyll content	[59]
SRPI = Simple Ratio Pigment Index	$(R430)/(R680)$	Carotenoid/chlorophyll-a content	[57]
WI = Water Index	$(R900)/(R970)$	Water status	[57]
PSRI = Plant Senescing Reflectance Index	$(R678–R500)/R750$	Leaf Senescence	[60]
mSR = modified Simple Ratio	$(R800–R445)/(R680–R445)$	Chlorophyll	[61]
VREI = Vogelmann Red-Edge Index	$(R734-R747)/(R715-R726)$	Chlorophyll concentration, canopy leaf area, and water content	[62]
REP = Red-Edge Position	$700 + 40 \frac{\frac{(R670+R780)}{2} - R700}{R740 - R700}$	Indicator of sharp change in leaf reflectance	[63,64]

R is used for reflectance at a specific wavelength in nm.

2.5. Statistical Analysis

2.5.1. Spectral Indices

A two-step statistical analysis was used to evaluate the potential of the various indices to discriminate plant species, whether at least one of them was statistically different for each index or not [47,65]. For this, null hypothesis, H0: μ1 = μ2, . . . , μ11 versus the alternative hypothesis, H1: μ1 ≠ μ2, . . . , μ11 was tested where μi is the mean indices values of each species (i species = 1, . . . , 11). So, the hypothesis test was carried out firstly by using one way-AVOVA (*p* < 0.05, *p* < 0.01, and *p* < 0.001) with each spectral index individually using Origin 2021 software. Secondly, multiple comparisons using post hoc test were carried out with those spectral indices that rejected the null hypothesis. Holm–Bonferroni test was applied using pairwise comparison plot app in Origin 2021 to determine which pairs of plant species (either native, introduced, or ornamental) were statistically different. The number of possible pairs combinations was calculated as n[(n − 1)/2], where n = number of species and equalled 55 [66]. The frequency of significant plant pairs was calculated in order to determine the most significant indices that showed the best discrimination between plant species.

2.5.2. Wavelength Spectra

One-way ANOVA was used to test for statistical differences between species at every spectral location between 325 nm and 1075 nm (a total of 751 spectral bands) with 95% confidence (*p* < 0.05) as it was important to identify the regions of the electromagnetic spectrum in which the species were significantly different from each other [38,41,67]. Prior to performing the ANOVA, normality and homoscedasticity (homogeneity of variances) of the reflectance values across each waveband were verified and bands with unequal variance were excluded. Rejection of the null hypothesis was followed by pairwise comparisons of plant species with post hoc Holm multiple tests using Jeffrey's Amazing Statistics Program (JASP) software version 14.1.0 (Netherlands) at each waveband. After that, the frequency of statistically significant pairs between 11 plant species (55 pairs) was counted per waveband, which allowed us to determine the most discriminating wavelengths. Histogram of significance frequencies per wavelength was made using Origin 2021. Comparative analysis of native and invasive species showing significant regions of electromagnetic spectrum were also plotted for better visualization.

2.6. Spectral Separability Analysis

Spectral separability analysis was calculated using the Jeffries Matusita (JM) distance that measures the average distance between each pair (55) of plant species in the multidimensional space defined by the wavelengths [37,68,69]. It was used to test the hypothesis that some spectral bands have more discriminatory power between species than others in an electromagnetic spectrum [70]. Being a parametric test, it was not possible to execute the JM distance calculation over the full spectrum of significant hyperspectral wavebands due to the singularity problem of matrix inversion [41]. Therefore, it was necessary to reduce the number of spectral features (wavebands) prior to the JM calculation. Thus, to reduce data dimensionality, bands with at least 17 significantly different plant pairs were chosen for separability analysis. The JM distance was computed for each plant pair (55) taking the fifteen selected wavelengths to determine the best combinations of bands for separating the classes. The JM distance value ranges between 0 and 2, with a larger JM distance value indicating higher separability between group pairs [71]. The equation of JM distance is:

$$JM_{ij} = 2\left(1 - e^{-B}\right) \tag{1}$$

where

$$B = \frac{1}{8}\left(\mu_i - \mu_j\right)^T \left(\frac{C_i + Cj}{2}\right)^{-1}\left(\mu_i - \mu_j\right) + 2\ln\left(\frac{\left(\frac{1}{2}\right)|C_i + C_j|}{\sqrt{|C_i|x|C_j|}}\right) \tag{2}$$

i and j = the two classes being compared, C_i = the covariance matrix of signature i, μ_i = the mean vector of signature i, ln = the natural logarithm function, $|C_i|$ = the determinant of C_i (matrix algebra), T = transposition function.

The R-statistical package [72] was used to measure JM distance using different bands to achieve the best band combinations that fully discriminate the native and invasive species [67]. To summarise the results, the JM values were averaged for all pairs with different band combinations [73,74]. Figure 4 presents a flowchart of the main steps and framework of the whole process.
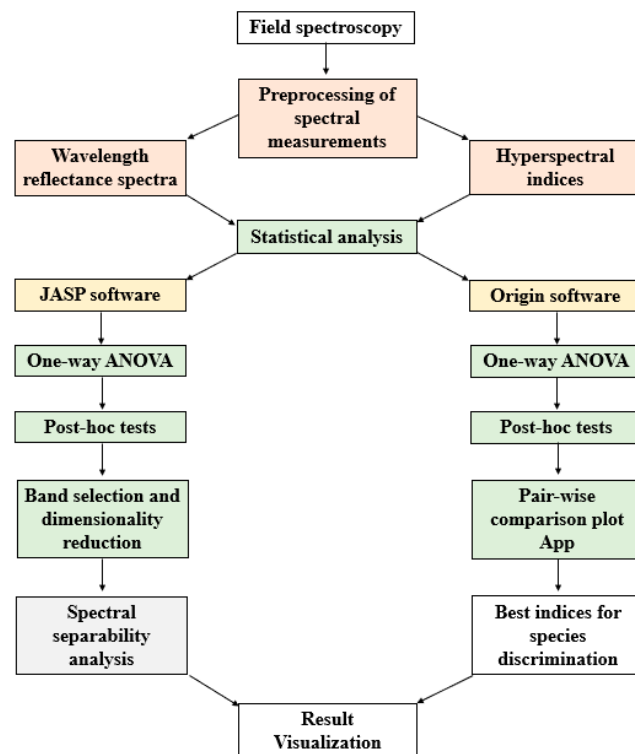

Figure 4. Flowchart of the main methodology adopted.

3. Results

3.1. Spectral Indices

Spectral curves of plant species showed sensitivity in different spectral regions according to their biophysical and biochemical characteristics. The analysis of one-way ANOVA showed significant differences ($p < 0.05$) with nine calculated spectral indices viz. REP, VREI, NDVI, PRI, WI, SRPI, LCI, GI, and GMI (Table 3). This result showed that most of the spectral indices had the ability to spectrally discriminate at least one pair of the plant species, thus accepting the alternate hypothesis. GMI, GI and LCI also showed significant differences among plant species at a 99% confidence level ($p < 0.01$). However, ANOVA showed the highest significant results for the red-edge indices, i.e., REP and VREI at 99.9% confidence level ($p < 0.001$). Only two spectral indices, mSR and PSRI, showed non-significant results ($p > 0.05$), hence supporting the null hypothesis (Table 3).

Table 3. Mean spectral indices (biophysical and biochemical parameters) of different plant species.

Plant Category	Plant Species	NDVI *	GMI **	GI **	PRI *	PSRI n.s	LCI **	WI ***	SRPI **	mSR n.s	REP ***	VREI ***
Ornamental	*Eucalyptus camaldulensis* (EC)	0.81	4.91	1.87	0	−0.02	0.626	1.013	1.043	20.73	721.73	0.78
	Pongamia pinnata (PP)	0.91	7.17	2.45	−0.04	0.01	0.713	1.029	0.738	78.66	723.03	0.854
	Tecoma stans (TS)	0.72	3.80	2.18	−0.07	0.15	0.462	1.024	0.555	53.28	719.26	0.563
	Callistemon viminalis (CV)	0.74	3.00	1.90	−0.05	0.03	0.455	1.042	0.663	23.02	717.54	0.503
Invasive	*Parthenium hysterophorus* (PH)	0.59	2.18	1.09	−0.06	0.10	0.387	1.012	0.443	6.67	718.14	0.638
	Prosopis juliflora (PJ)	0.74	3.78	1.53	−0.06	0.03	0.542	1.044	0.676	31.59	720.79	0.639
	Leaucena leucocephala (LL)	0.77	3.48	1.79	−0.03	0.02	0.516	0.918	0.546	18.29	719.1	0.540
	Lantana camara (LC)	0.79	3.97	1.74	−0.06	0.02	0.544	1.011	0.706	34.86	719.47	0.503
Native	*Justicia adhatoda* (JA)	0.89	5.52	2.80	−0.01	0.003	0.642	1.080	0.807	93.63	721.54	0.741
	Acacia modesta (AM)	0.80	3.92	2.34	−0.03	−0.001	0.524	1.001	0.833	123.13	718.27	0.478
	Dodonea viscosa (DV)	0.78	3.67	1.75	−0.06	0.038	0.528	1.001	0.504	16.65	719.23	0.565

ANOVA significance level: * = $p < 0.05$, ** = $p < 0.01$, *** = $p < 0.001$, n.s = non-significant.

Following the ANOVA, multiple comparisons of plant species using Holm–Bonferroni tests subsequently explained which pairs of plant species (total 55 pairs) showed spectral discrimination based on the calculated spectral indices. Among all indices, the red-edge indices, i.e., REP and VREI showed the highest potential to discriminate between pairs of plant species (Figure 5). For example, 32 pairs (58%) of plant species were able to be discriminated using REP (Figure 5a), out of which 14 species pairs showed a high significance level for discrimination ($p < 0.001$). Similarly, 28 pairs (51%) of plant species were significantly different from each other when using VREI (Figure 5b). The simple ratio pigment index (SRPI) was also able to distinguish 18 pairs (33%) of plant species (Figure 5c). However, NDVI showed the lowest potential to discriminate species and was able to differentiate only 11 pairs (20%) of plant species (Figure 5d).
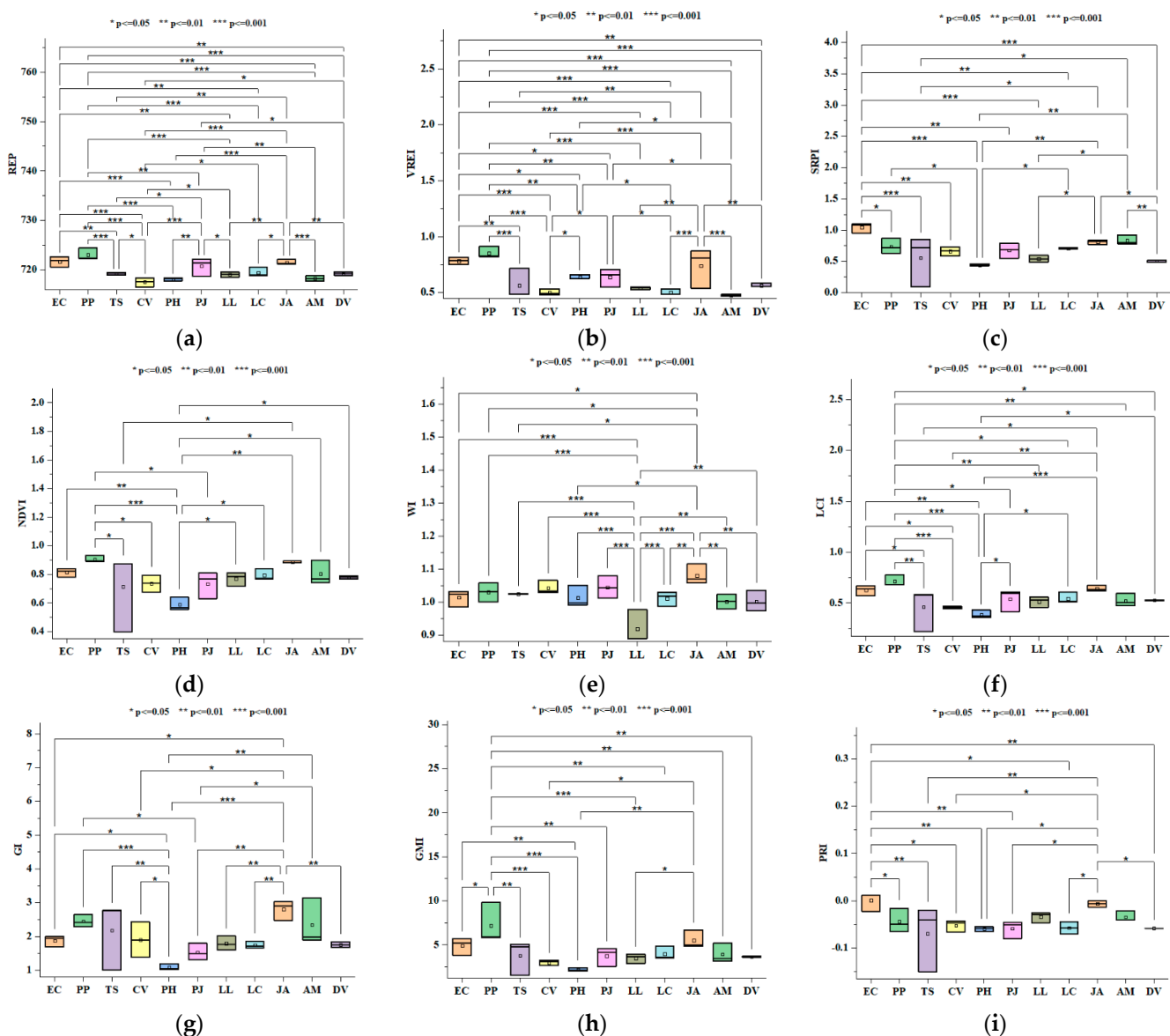

Figure 5. Pairwise comparison of significant spectral indices REP (**a**) VREI (**b**) SRPI (**c**) NDVI (**d**) WI (**e**) LCI (**f**) GI (**g**) GMI (**h**) and PRI (**i**). The lines above boxplots indicate only the significant pairs at 0.05 (*), 0.01 (**) and 0.001 (***) significance level among different pairs of plant species. The abbreviations of plant species on the x axis are mentioned in Table 2.

The Water Index (WI) was also better than other spectral indices in showing spectral separability among 17 pairs (31%) of plant species (Figure 5e). LCI, GI, GMI and PRI showed successful discrimination of 17 (31%), 14 (26%), 13 (24%) and 13 (24%) pairs of

plant species, respectively (Figure 5f–i). However, out of 55 pairs of plant species, PRI did not show any pairwise significance at the 99.9% confidence level, hence indicating less potential for discrimination than other indices (Figure 5f).

Some plant species pairs showed significant differences with all spectral indices ($p < 0.05$). For instance, *P. hysterophorus* (invasive) was able to be discriminated from *J. adhatoda* (native), *E. camaldulensis* (ornamental) and *P. pinnata* (ornamental) pairs with 78–88% of all the indices (Figure 5). Similarly, *T. stans* (ornamental) also showed discrimination of 78% with all indices when compared with *J. adhatoda* (native). However, it was not possible to discriminate *A. modesta* (native) from *L. camara* (invasive) and *C. viminalis* (ornamental) at any of the spectral indices ($p > 0.05$) during pairwise comparisons. Similarly, *L. camara* (invasive) showed non-significant results with *D. viscosa* (native) and *T. stans* (ornamental) at a 95 % confidence level (Table A1).

A unique trend was observed when the percentage discrimination was studied for individual plant species with reference to any specific vegetation index. Each plant species had a different level of sensitivity towards each vegetation index. For example, *P. pinnata* (PP) was significantly different from nine other plant species using the GMI index (Figure 6). By using water index, *L. leucocephala* (LL) was successfully discriminated from all 10 plant species. Similarly, *J. adhatoda* was discriminated from eight plant species using WI (Figure 6). However, *P. hysterophorus* (PH) was more sensitive towards NDVI than all other indices and discrimination from seven plant species (Figure 6). Likewise, *E. camaldulensis* was able to discriminate from eight plant species using SRPI index. Interestingly, *A. modesta* (AM) and *L. leucocephala* (LL) were not able to differentiate from any plant species using PRI (Figure 6).

3.2. Wavelength Spectra

The spectral signatures of the 11 plant species were observed in plots of wavelength versus reflectance (Figure 7a). The visual pattern of the mean reflectance of all species look similar to a typical vegetation curve. However, detailed illustration (zoom regions) of plant species revealed different features and crossovers across wavelength regions in the visible, red-edge, and NIR regions (Figure 7b–d). The differences in the absorption strength were more pronounced visually in the NIR regions, especially in the case of *L. leucocephala* (invasive) vs. *D. viscosa* (native) and *P. pinnata* (ornamental) vs. *P.hysterophorus* (invasive). Generally, it was observed that the tree species (*L. leucocephala*, *P. pinnata*, *P. juliflora*) showed higher reflectance values (0.56–0.78) in the leaf spectra than the reflectance (0.38–0.48) of small shrubs or herbs (*L. camara*, *D. viscosa*, *P. hysterophorus*) in full spectrum (Figure 7).

The one-way ANOVA with individual wavebands showed that results were statistically significant ($p < 0.05$), supporting that at least one species was significantly different from one other species in terms of spectral reflectance at that wavelength. Hence, many individual wavebands supported alternate hypothesis (Table 4). Out of the 751 wavebands (325–1075 nm), significant differences were observed in 562 wavebands (75% frequency). These significant wavelengths were located in three different regions of the electromagnetic spectrum (visible, red-edge and near-infrared). However, the NIR region contributed most (96%, $n = 313$) to the spectral discrimination of all plant species (Table 4). The p-value ($p < 0.05$, $p < 0.01$, $p < 0.001$) plot has shown the wavelength regions that were spectrally separable (Figure 8).

The graphical representation of the ANOVA outcomes showed that most of the regions of leaf spectra were statistically different for all plant species (Figure 9). Most of the red-edge and NIR regions were able to show spectral differences among all plant species. The reflectance curves at blue wavelengths in the visible region also showed significant differences ($p < 0.05$). However, it was evident that 189 wavelength bands located in red and red-edge regions had statistically non-significant ANOVA ($p > 0.05$) results (Figure 8), indicating that these regions (582–699 nm) were similar in reflectance among all plant species (Figure 9).
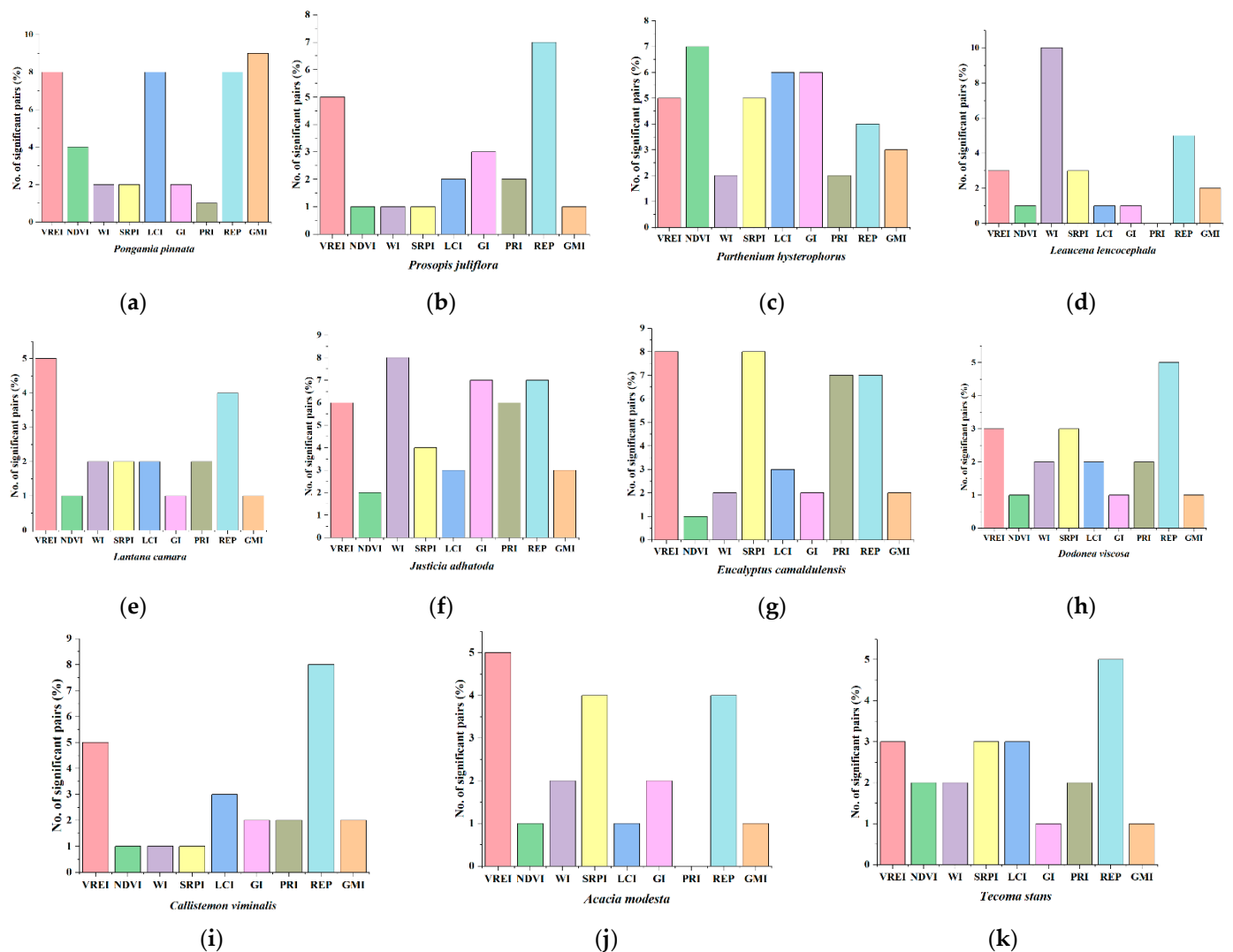
Figure 6. Graphical representation of individual plant species (**a**–**k**) showing the potential of discrimination with significant pair of species using different spectral indices.

The Holm post hoc multiple tests resulted in 55 possible pair combinations for the 11 plant species. Pairwise comparisons of all plant species showed that different species pairs were significantly different at several wavelength regions. Table 5 shows the frequency of the significant bands adapted into the three spectral domains. It was observed that LL vs. DV (invasive vs. native) was the most significant pair, with 505 wavelengths bands (67 %) that were statistically different and located all over the spectral regions (Table 5). The significant wavelengths for the pair EC vs. PP (ornamental vs. ornamental) were located only in the visible portion (325–680 nm) of the electromagnetic spectrum (*n* =137). Similarly, the pair LC vs. PP (invasive vs. ornamental) was statistically different (*n* = 4) only in the near-infrared wavelength region (Table 5). However, some of the pairs of plant species showed non-significant results over the whole spectrum., i.e., LC vs. AM (invasive vs. native), LC vs. JA (invasive vs. native), PH vs. AM (invasive vs. native), AM vs. CV (native vs. ornamental). Overall, 46 plant pairs (84%) showed discrimination in the visible region, while 33 plant pairs (60%) were able to be discriminate from one another in the NIR region (Table 5).
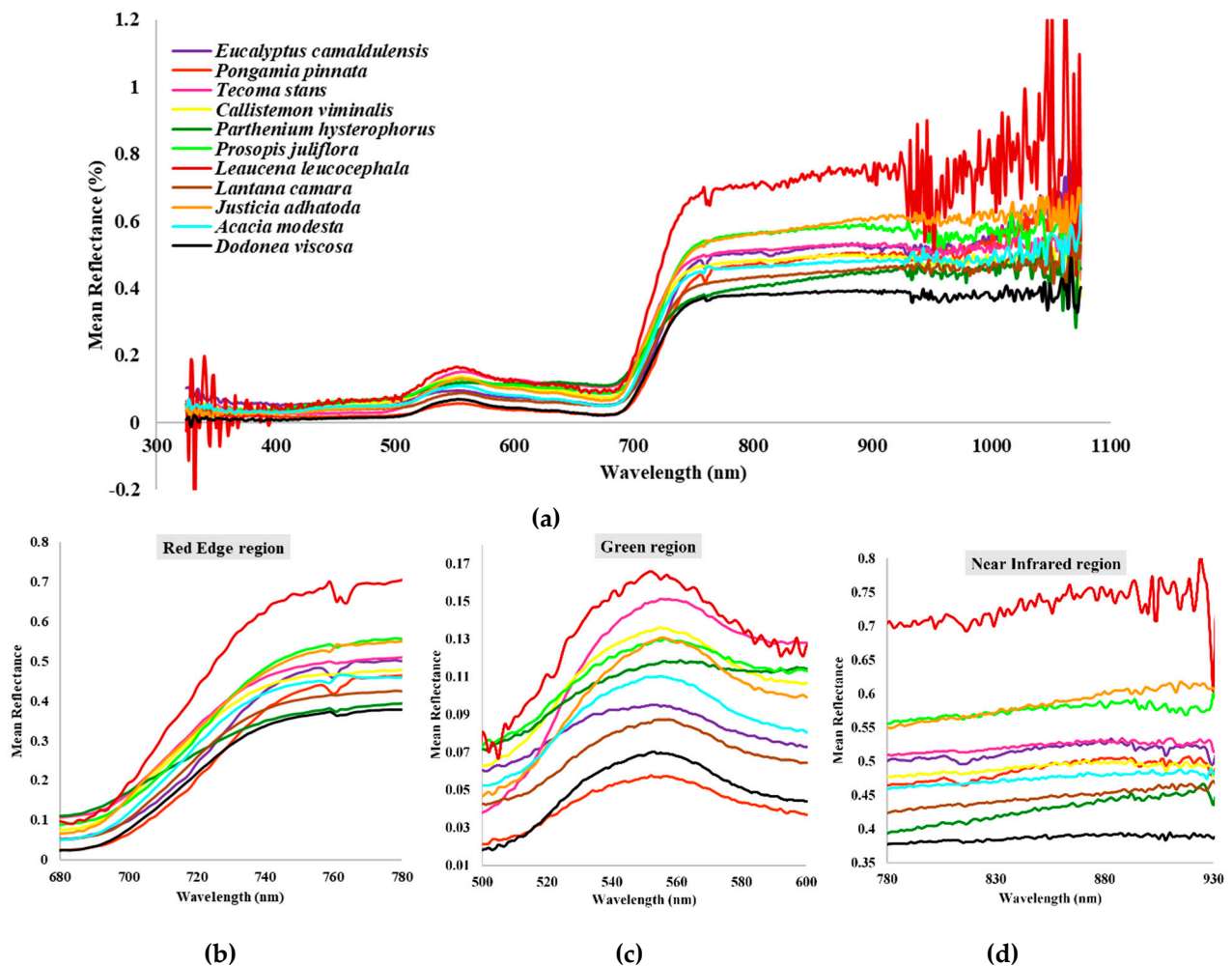
Figure 7. Spectral signatures of all plant species showing mean reflectance (**a**), green (**b**), red-edge (**c**) and NIR region (**d**).

Table 4. Frequency of significant wavebands in different regions of electromagnetic spectrum based on ANOVA ($p < 0.05$).

Wavelength Region	Description	Total No. of Bands	Significant Bands ($p < 0.05$)	Non Significant Bands	Frequency
325–680 nm	Visible region	356	199	157	56%
681–750 nm	Red-edge region	70	50	20	71.4%
751–1075 nm	NIR region	325	313	12	96%
325–1075 nm	Whole spectrum	751	562	189	75%

For illustrative purposes, twelve pairs of plant species (invasive vs. native) were selected for comparisons (Figure 10). *Leucaena leucocephala* was one of the invasive trees in Jindi Reserve Forest that showed significant variations for all three native species at different wavelengths, especially in 218 selected bands (709–927 nm) of the NIR region (Figure 10a). *Prosopis juliflora* (PJ) was able to be discriminated from *D. viscosa* (DV) at most of the red-edge and NIR wavelengths (Figure 10b). However, the pair PJ vs. AM was only significantly different at 341 nm (visible region). *Lantana camara* exhibited less discrimination ability with wavelength spectra than other invasive plant species and was able to be discriminated only from one of the native species, *D. viscosa*, at a few NIR wavelengths (Figure 10c). Interestingly, *P. hysterophorus* showed the most discriminating wavebands in the visible regions of spectrum but it was not possible to discriminate this herbaceous weed from *A. modesta* at any spectral band (Figure 10d).
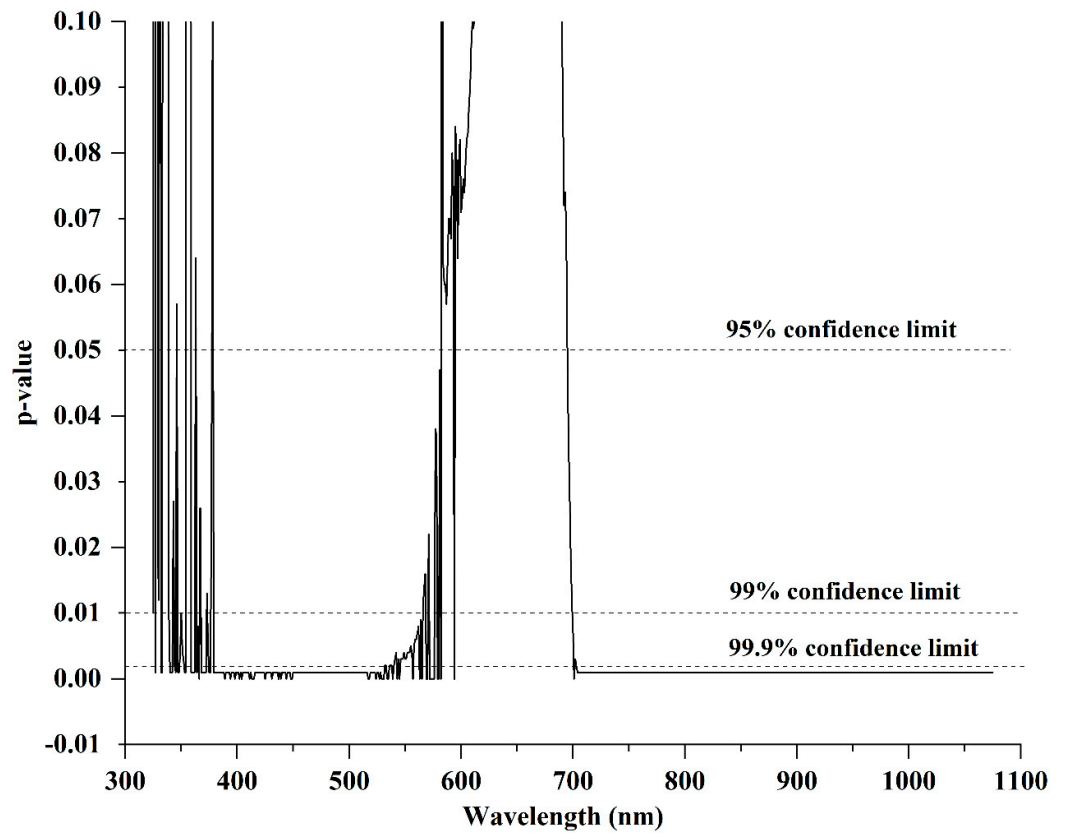
Figure 8. Significance value plot of the ANOVA test. The *p*-value shows that the mean reflectance of all species at every spectral band ($n = 562$) is significantly different ($p < 0.05$).
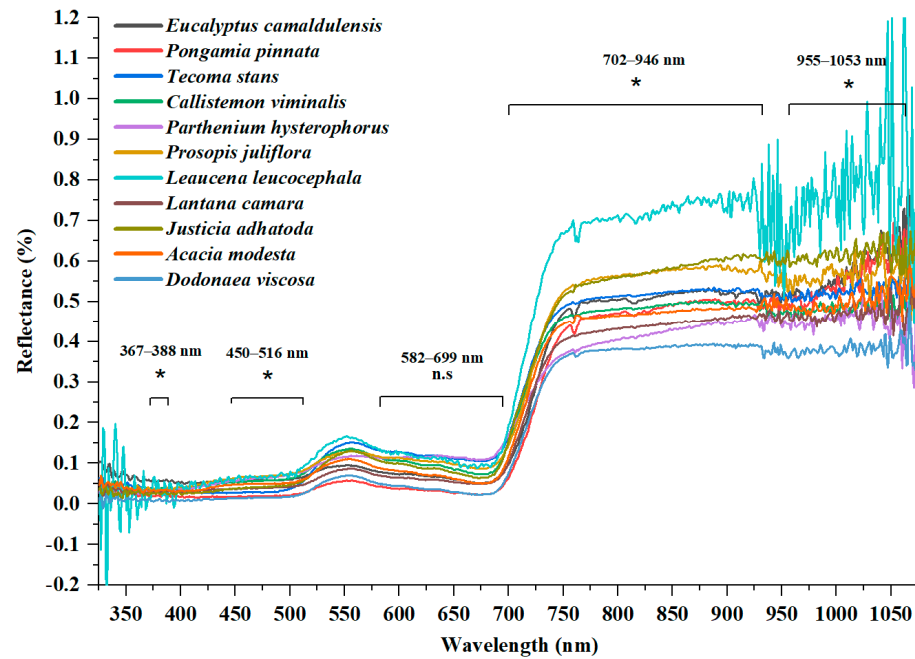

Figure 9. Graphical representation of discriminating wavebands ($p < 0.05$) among plant species through ANOVA in different regions of spectrum.

Table 5. Pairwise comparisons of all plant species (55 pairs) showing the frequency of significant wavelength bands in different regions of reflectance spectra. Values in parentheses represent percentage (%) of significant bands.

Plant Category	Plant Pairs	Significant Bands (%)			
		Visible 325–680 nm	Red-Edge 681–750 nm	Near Infrared 751–1075 nm	Full Spectrum 325–1075 nm
Invasive	LC vs. AM	0 (0)	0	0	0
	LC vs. CV	2 (0.56)	0	6 (1.85)	8 (1.07)
	LC vs. DV	1 (0.28)	0	11(3.38)	12 (1.60)
	LC vs. EC	48 (13.48)	0	0	48 (6.39)
	LC vs. LL	84 (23.60)	46 (65.71)	284 (87.38)	414 (55.13)
	LC vs. PH	7 (1.97)	0	0	7 (0.93)
	LC vs. PJ	68 (19.10)	0	0	68 (9.05)
	LC vs. PP	0	0	4 (1.23)	4 (0.53)
	LC vs. TS	0	0	0	0
	LC vs. JA	0	0	0	0
	LL vs. JA	122 (34.27)	47 (67.14)	258 (79.38)	427 (56.86)
	LL vs. CV	25 (7.02)	35 (50.00)	277 (85.23)	337 (44.87)
	LL vs. DV	150 (42.13)	48 (68.57)	307 (94.46)	505 (67.24)
	LL vs. EC	36 (10.11)	47 (67.14)	257 (79.08)	340 (45.27)
	LL vs. PH	26 (7.30)	40 (57.14()	290 (89.23)	356 (47.40)
	LL vs. PJ	28 (7.87)	36 (51.43)	126 (38.77)	190 (25.30)
	LL vs. PP	160 (44.64)	50 (71.43)	262 (80.62)	472 (62.85)
	LL vs. TS	108 (30.34)	31 (44.29)	267 (82.15)	406 (54.06)
	LL vs. AM	27 (7.58)	42 (60.00)	278 (85.54)	347 (46.21)
	PH vs. AM	0	0	0	0
	PH vs. CV	1 (0.28)	0	1 (0.31)	2 (0.27)
	PH vs. DV	104 (29.21)	0	6 (1.85)	110 (14.65)
	PH vs. EC	26 (7.30)	0	10 (3.08)	36 (4.79)
	PH vs. PJ	0	2 (2.86)	62 (19.08)	64 (8.52)
	PH vs. PP	106 (29.78)	0	3 (0.92)	109 (14.51)
	PH vs. TS	75(21.07)	0	1 (0.31)	76 (10.12)
	PH vs. JA	84 (23.60)	0	0	84 (11.19)
	PJ vs. AM	1 (0.28)	0	0	1 (0.13)
	PJ vs. JA	95 (26.69)	0	0	95 (12.65)
	PJ vs. CV	1 (0.28)	0	0	1 (0.13)
	PJ vs. DV	116 (32.58)	38 (54.29)	284 (87.38)	438 (58.32)
	PJ vs. EC	6 (1.69)	0	1 (0.31)	6 (0.08)
	PJ vs. PP	117 (32.87)	18 (25.71)	1 (0.31)	136 (18.11)
	PJ vs. TS	84 (23.60)	0	0	84 (11.19)
Native	AM vs. PP	79 (22.19)	0	0	79 (10.52)
	AM vs. TS	0	0	0	0
	AM vs. JA	3 (0.84)	0	0	3 (0.40)
	AM vs. CV	0	0	0	0
	AM vs. DV	24 (6.74)	22 (31.43)	79 (24.31)	125 (16.64)
	AM vs. EC	32 (8.99)	0	1 (0.31)	3 (0.40)
	JA vs. CV	40 (11.24)	0	0	40 (5.33)
	JA vs. TS	1 (0.28)	0	0	1 (0.13)
	JA vs. DV	1 (0.28)	26 (37.14)	270 (83.08)	297 (39.55)
	JA vs. EC	111 (31.18)	0	4 (1.23)	115 (15.31)
	JA vs. PP	0	0	0	0
	DV vs. CV	110 (30.90)	42 (60.00)	202 (62.15)	354 (47.14)
	DV vs. EC	132 (37.08)	12 (17.15)	294 (90.46)	438 (58.32)
	DV vs. PP	2 (0.56)	0	212 (65.23)	214 (28.50)
	DV vs. TS	7 (1.97)	44 (62.86)	261 (80.31)	312 (41.54)
Ornamental	CV vs. EC	8 (2.25)	0	0	8 (1.07)
	CV vs. PP	119 (33.43)	19 (27.14)	4 (1.23)	142 (18.91)
	CV vs. TS	61 (17.13)	0	0	61 (8.12)
	EC vs. PP	137 (38.48)	0	0	137 (18.24)
	EC vs. TS	89 (25.00)	6 (8.57)	2 (0.62)	97 (12.92)
	PP vs. TS	21 (5.90)	26 (37.14)	2 (0.62)	49 (6.52)

The histogram (frequency analysis) represented the number of plant species pairs that were significantly different at each waveband. The maximum frequency of significant pairs was 27 (approx. 50%) at the 390 nm wavelength. However, the minimum count of statistically different pairs was 1 (approx. 2%) at a few spectral bands of 558–562 nm wavelengths (Figure 11). The 15 spectral bands of the most significant wavelengths were

selected for further separability analysis, and these bands were located in the visible, red-edge and NIR regions (Table 6).
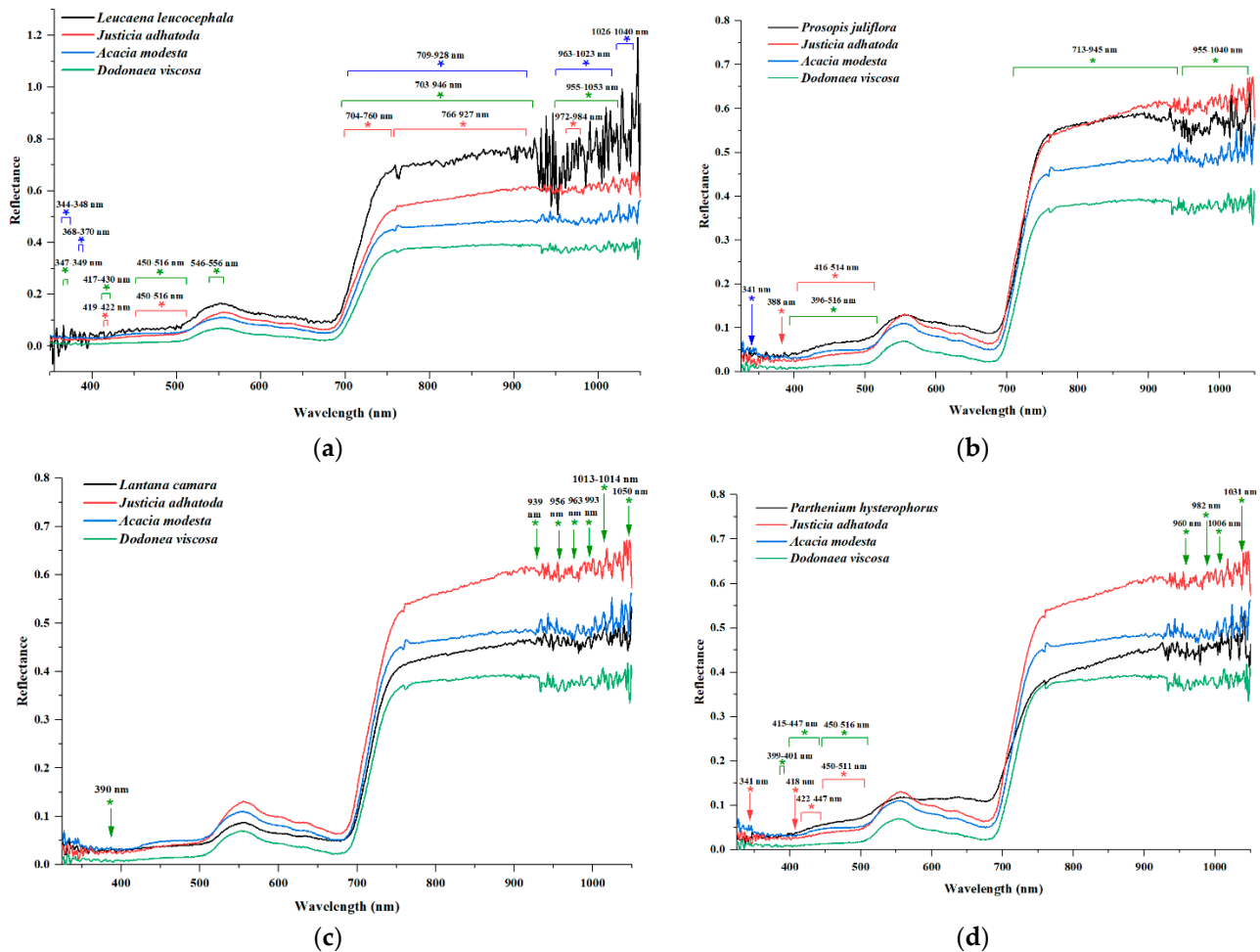

Figure 10. Graphical representation of pairwise comparisons of plant species. Each graph shows comparative analysis of native vs. invasive species spectra. Bars and arrow represent the significant discriminating wavebands with one of the invasive species, *L. leucocephala* (**a**) *P. juliflora* (**b**) *L. camara* (**c**) and *P. hysterophorus* (**d**) in each graph.

3.3. Jeffries–Matusita Distance Analysis

The JM distance values for most of the plant species pairs were greater than 1.9 with different band combinations. Table 7 shows the JM analysis averaged for all combined pairs of plant species. The results also revealed that use of more bands improved the separability of the different species., i.e., the two band combinations of 390 and 451nm had an average JM value of 1.094 while the combination of four bands (390, 432, 433 and 450 nm) showed a higher JM value of 1.345 (Table 7). Similarly, the band combination of 1014 and 1037 nm (NIR region) had an average JM value of 1.478, while the combination of three bands (1013, 1014 and 1037 nm) showed a higher JM value of 1.515. However, a trend of a decrease in the average JM value was observed when the band combinations from three different spectral regions (visible, red-edge and NIR) were used together for calculating spectral separability (Table 7).

Table 8 shows the JM distance values for each individual plant species (55 pairs) with one of the best band combinations (724 nm and 725 nm). It produced best separability value of 2 (100%) with 28 pairs of plant species and almost 44 plant pairs showing acceptable JM value of more than 1.90., i.e., *L. camara* vs. *A. modesta* (invasive vs. native) had a JM distance of 1.98. Similarly, the pair *P. hysterophorus* and *J. adhatoda* (invasive vs. native) reached a

total separability of 2 (100%). However, some other plant pairs (*P. juliflora* vs. *C. viminalis* and *P.juliflora* vs. *J. adhatoda*) did not achieve total separability even by using the same two bands (Table 8).
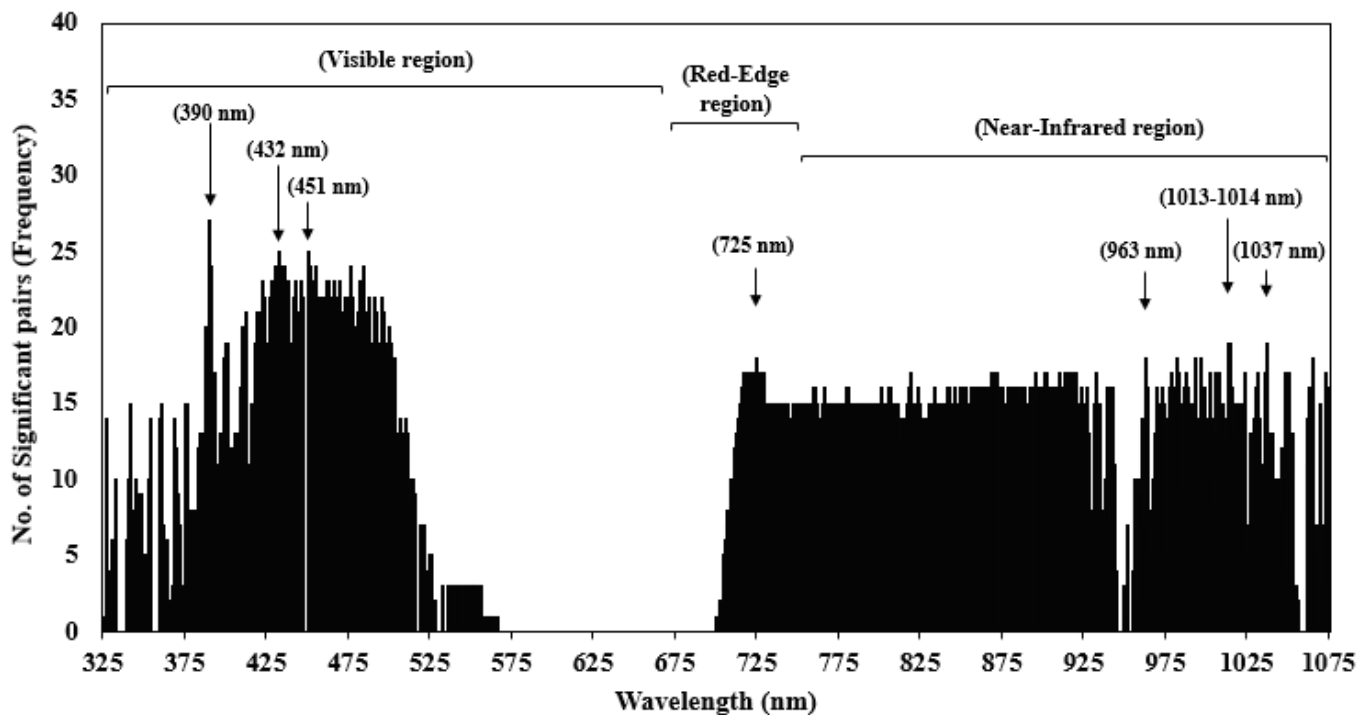

Figure 11. Histogram of reflectance spectra per wavelength showing significant frequencies with pairs of plant species. Some highest frequencies in Visible, red-edge and NIR regions are indicated with arrows.

Table 6. A few of the most significant wavelength bands selected from ANOVA, based on the maximum number of significant pairs (frequencies) at each wavelength.

Spectrum Region (325–1075 nm)	Wavelengths Selected (nm)	No. of Most Significant Wavelengths
Visible region (325–680 nm)	390, 432, 433, 451	4
Red-edge region (681–750 nm)	721, 724, 725	3
Near-infrared region (751–1075 nm)	963, 982, 993, 996, 1013, 1014, 1037, 1075	8

Table 7. The averages of JM distance analysis for all pairs of plant species (55). The symbol (×) indicates the selection of optimal bands in each band combination.

Band Combinations	Visible Region (nm)				Red-Edge Region (nm)						NIR Region (nm)					Average JM Value	%
	390	432	433	451	721	724	725	963	982	993	996	1013	1014	1037	1075		
2 bands (V)	×			×												1.094	54.7
2 bands (R)						×	×									1.714	85.45
2 bands (NIR)													×	×		1.478	73.9
3 bands (V)	×	×		×												1.255	62.75
3 bands (R)					×	×	×									1.387	69.35
3 bands (NIR)												×	×	×		1.516	75.8
3 bands (VRN)	×						×							×		0.056	2.8
4 bands (V)	×	×	×	×												1.345	67.25
4 bands (RN)						×	×						×		×	0.401	20.05
4 bands (NIR)												×	×	×	×	1.323	66.15
4 bands (VRN)	×			×			×							×		0.048	2.4
5 bands (VRN)	×	×		×		×	×									0.043	2.15
6 bands (VRN)	×			×	×	×						×	×			0.072	3.6

Table 7. *Cont.*

Band Combinations	Visible Region (nm)				Red-Edge Region (nm)			NIR Region (nm)								Average JM Value	%
7 bands (VR)	×	×	×	×	×	×	×									0.061	3.05
8 bands (NIR)								×	×	×	×	×	×	×	×	1.265	63.25
9 bands (RN)							×	×	×	×	×	×	×	×	×	0.584	29.2
9 bands (VRN)	×		×	×	×	×	×			×			×			0.058	2.9
10 bands (VRN)	×		×	×	×	×	×		×			×	×			0.067	3.35
11 bands (RN)					×	×	×	×	×	×	×	×	×	×	×	0.061	3.05
12 bands (VN)	×	×	×	×				×	×	×	×	×	×	×	×	0.071	3.55
15 bands (VRN)	×	×	×	×	×	×	×	×	×	×	×	×	×	×	×	0.0067	0.335

V = visible, R = red-edge, NIR = near infrared, VN = visible and near-infrared, VR = visible and red-edge, RN = Red-edge and near infrared, VRN = visible, red-edge and near-infrared.

Table 8. The JM distance between 11 plant species using two bands (724 and 725 nm). The species pairs having a separability level below the threshold (JM index of 1.90) are highlighted.

	EC	PP	TS	CV	PH	PJ	LL	LC	JA	AM	DV
EC	0	1.952	2	1.999	0.230	1.999	2	0.257	1.999	1.974	1.958
PP		0	2	2	1.997	2	2	1.998	2	2	0.275
TS			0	1.570	2	0.702	2	2	0.278	1.997	2
CV				0	2	0.299	2	1.999	0.881	1.682	2
PH					0	2	2	0.359	2	1.999	1.999
PJ						0	2	1.999	0.1801	1.751	2
LL							0	2	2	2	2
LC								0	2	1.984	1.999
JA									0	1.959	2
AM										0	2
DV											0

4. Discussion

Early detection of invasive alien plants and the ability to discriminate them from native vegetation in protected areas is critical for land managers to devise timely management interventions. Hyperspectral remote sensing is an effective tool to monitor and discriminate plant invasions at species level across a range of habitats, based on spectral properties [75,76]. Several studies have used field-based instruments as well as hyperspectral satellite images to distinguish and map alien species from other co-existing native species [39,42]. Field spectroscopy is mainly used for the evaluation of biophysical and biochemical properties to discriminate species independently, without any attempt to integrate the analytical techniques for species mapping [7,77]. The aim of this research was to evaluate the potential of field spectroscopy to discriminate native and invasive plant species in Lehri and Jindi Reserve forests. Different narrow-banded hyperspectral indices and diagnostic wavelength regions were identified using reflectance data, having the potential to differentiate plant species as well as the distance among each pair of plant species to find out the spectral separability between them.

Most of the spectral vegetation indices were able to discriminate between the native and invasive plant species at leaf level (Figure 5). This was possible due to the variations existing in the leaf pigments, intercellular spaces, water content, cell wall thickness, cell size, and other structural and biochemical properties of different plant species [42,78]. Among spectral indices, both red-edge parameters (REP and VREI) showed the highest potential for identifying pairs of plant species (Figure 5a,b). The red-edge region is the transition zone connecting the red and near infrared regions (680–750 nm) which acts as an indicator of sharp leaf reflectance change and is sensitive to chlorophyll concentration [64,79]. Cho et al. [47] demonstrated that REP has the potential to spectrally discriminate different plant species and it is not sensitive to atmospheric conditions [80]. Recent studies have shown better discrimination of vegetation species using red-edge algorithms [65,81].

The NDVI showed the lowest potential to identify plant species, with only 20% of results being significant, and was able to differentiate only 11 pairs of plant species (Figure 5d). NDVI is the indicator of photosynthetic capacity and linked with the health of vegetation [82,83]. The possible reason might be the season of spectral data collection, which for this study was the start of autumn. Bratsch et al. [84] reported that NDVI is more useful for separating plant communities at the peak growing season, and it may be problematic during the early or late growing season, due to similar spectral responses of vegetation. Two indices, mSR and PSRI, were not able to differentiate any native or invasive plant species (Table 3). mSR is the spectral index related to prolonged chlorophyll stress in the canopy structure [85] and PSRI is the indicator of leaf senescence stage and is sensitive to the carotenoid/chlorophyll ratio [86]. It seems that reflectance values at the wavelengths 445, 500, 678 and 800 nm, used to measure both indices, did not show much variability and thus could not support species level identification. Previous studies used different hyperspectral indices to check the potential of identification of invasive species or other vegetation species [48,87], therefore it is difficult to relate each finding with the literature due to high variability in the growth and habit of plant species.

Among plant species (either native, invasive, or ornamental), the level of spectral sensitivity towards each spectral index varied individually., i.e., *L. leucocephala* was able to be discriminated from all other plant species using the Water index (Figure 6). The reason may be the unique reflectance of *L. leucocephala* at 900 and 970 nm wavelengths that resulted in the 100% spectral separability. Another reason could be the water stress variations within all species of the forest due to the ground water availability in the autumn season that may successfully discriminate taxa at species level [88]. However, the same species, *L. leucocephala*, was unable to be differentiated from all other co-existing species using the PRI index (Figure 6). *Lantana camara* also showed higher differentiation with other co-existing species using VREI index. Similarly, *P. hysterophorus* was best discriminated from all other native and introduced plant species using NDVI (670 and 830 nm wavelengths), even though the overall potential of NDVI to differentiate plant species was considered low (Figure 5d). Kganyago et al. [89] also showed better discrimination of *P. hysterophorus* using red-edge and NIR spectral bands in South Africa. All these highly variable findings with different species suggest that it is not feasible to use one spectral index universally for the discrimination of all plant species.

The analysis of wavelengths spectra through ANOVA confirmed the successful spectral separation of native and invasive plant species in the visible, red-edge and NIR regions through field measurements. A number of significant wavebands (562) eventually support the fact that significant variations exist between the plant species studied in Lehri and Jindi Reserve forests. However, wavebands in NIR region (751–1075 nm) contributed the most ($n = 313$) in the discrimination in current study (Figure 9). These results agree with previous studies where leaf spectra have shown the greatest variation in the near-infrared and red-edge regions [37,90,91]. Significant wavelengths in the red-edge region (680–750 nm) may be due to the variations in chlorophyll concentration, nitrogen concentration, and water content between different species [92,93]. However, few wavelength regions at 582–699 nm (Figure 9) showed non-significant results ($p > 0.05$), which depicts the underlying similarities in physiological and biochemical characteristics among different plant species [89]. Another reason may be the greater intraspecific variability than interspecific variability in these regions. Similar results were obtained when identifying invasive species of Virginia state, USA through field spectroscopy where the 550–599 and 650–699 nm regions were not able to support plant identification [42]. Previous studies also indicated that not all bands can be important in species identification [41]. Therefore, it is feasible to use ANOVA for analysing the entire spectral profile rather than selecting only few narrow bands (indices) in order to achieve better detection of plant chemical composition [94]. It also showed the capability of the technique to reduce dimensionality by filtering the redundant bands and retaining only the informative bands after screening [38].

Pairwise comparison of plant species showed discrimination at several wavelength regions depending upon variability in individual plant species (Figure 10; Table 5). This was expected because the ability to identify spectra depends on spectral variability within and across the individual species [95]. Each species, either native or invasive, has a unique spectral signature, different from the other species and that is the core idea of the current study. Although ANOVA showed the NIR region has contributed the most to the identification of plant species ($n = 313$), the post hoc tests based on pairwise comparisons (55 pairs) discriminated more plant species pairs within visible regions (84%) than the NIR regions (60%; Table 5). These results indicate the importance of visible region (325–680 nm) in terms of spectral identification of plant species. Ferreira et al. [66] also showed similar findings and screened visible region hyperspectral bands as the most significant wavelengths for discriminating the tropical tree species. Visible reflectance at the leaf level is mostly a function of the pigment content [96]. Previous studies indicate that blue and red regions can be linked to variations in light absorption by plants. Thenkabail et al. [97] also screened six visible bands (490, 520, 550, 575, 660, 675 nm) for the identification of the plant species that were best at discrimination. The histogram of wavelength spectra also showed the highest frequency of significant pairs (50%) at 390 nm waveband (visible region). These results are in accordance with Schmidt and Skidmore [40] who found that the 404 nm waveband was useful for the spectral discrimination of plant species in the Netherlands.

Fifteen wavebands (390, 432, 433, 451, 721, 724, 725, 963, 982, 993, 996, 1013, 1014, 1037, 1075) were selected in this study for JM distance analysis, based on the highest frequency of significant pairs (Table 6). Previous studies also revealed that similar wavelength regions that are used for the discrimination among plant species in arid regions. Lewis [98] demonstrated that 720 nm wavebands and above were helpful in identifying some Australian arid region species. Similarly, Smith and Blackshaw [99] selected the 720–730 nm region as the most significant band in species differentiation. This may be because reflectance in this region is influenced by nitrogen, phosphorus, and potassium concentrations [100]. In the case of NIR wavebands, a similar waveband 986 nm was found to be useful for identifying species in a tropical dry forest [40]. This is perhaps due to the variations in the moisture content among different plant species that help in better discrimination [87].

The JM distance analysis revealed the spectral separability between pairs of plant species. Regions of red-edge and NIR with 2 and 3 band combinations, respectively (Table 7) were proven to be the best bands for separating the pairs of plant species. According to the literature, the separability between a pair is considered good when the JM distance is >1.9 and a pair is considered to be poorly separated if JM distance is <1.0 [101]. Almost 80% of plant species pairs, including native vs. invasive species pairs, were separable at >1.90 JM value with a two-band combination of 724 and 725 nm (Table 8). Previous studies also supported the findings of the JM separability index that some combinations of wavebands are more discriminating than others [35,40,41,74]. It was noted that the JM value decreased by using the band combinations from different regions of the spectrum (Table 7). The most valid reason may be the parametric nature of JM distance analysis that assumes the normal distribution of data [102]. The reflectance of each plant species varies greatly across visible, red-edge and NIR regions, ultimately resulting in poor JM separability if such wavebands from different regions are combined. However, the most interesting aspect was that some of the plant species pairs were not able to be separated with any spectral indices (Figure 5) as well as individual wavebands (Table 5), but the JM distance showed 99% spectral separability with the same pairs (Table 8)., i.e., *L. camara* (invasive) vs. *A. modesta* (native) was not possible to discriminate using spectral indices and wavelength spectra, but the JM distance between them was 1.98. The same observations were recorded for *P. hysterophorus* vs. *A. modesta*. These findings emphasize the importance of using band combinations in JM analysis that successfully discriminated all the species [103–105]. All previous discussion and current findings support the fact that it is possible to identify and ultimately map the distribution of invasive species through hyperspectral measurements.

5. Conclusions

This study aimed to investigate the potential of field spectroradiometer data for discriminating invasive species from other co-existing native species in the two protected scrub forests of Punjab, Pakistan. Our findings are promising, indicating the potential of applying statistical techniques to hyperspectral data in identifying invasive alien species of forests. It was observed that all plant species have characteristic spectral signatures that are distinguishable in many regions of the spectrum. Both leaf spectra and spectral indices suggest that wavelengths in the red-edge and near-infrared regions have a maximum potential to detect variations among all plant species, thus, a better understanding has been gained about those parts of the electromagnetic spectrum which offer the greatest information about discriminating between species pairs or groups. It concludes that not all of the indices contribute equally in the spectral discrimination of plant species. The red edge indices, i.e., REP and VREI have the highest potential to discriminate between pairs of plant species. Similarly, JM distance analysis indicated that the red-edge band combinations had the highest spectral separability at 724 and 745 nm wavelengths. Based on these findings, it is important to use and upscale this hyperspectral data to spaceborne or airborne high-resolution satellite images to map the distribution of invasive species in the Lehri and Jindi Reserve Forests. Although the results suggest a great potential for mapping invasive species through imaging remote sensing, further investigations are needed on the phenology of the plant species in different seasons that offer great variability and can influence the spectral separability of species. It is expected that multi-seasonal studies can explore the best timeframe for species-level mapping more precisely. Similarly, the spectral discrimination of invasive species can be improved by using first and second derivatives of spectra, hence further research is needed in this area to best distinguish different plant species. It is also worth noting that the spectral signatures of plant species in the current study are representative of this specific habitat and may not provide sufficient information for plant discrimination across the whole of Pakistan due to its high climactic variability. Moreover, the collection of more field spectral signatures within different zones of forests is also recommended to find more spectral diversity within individual species as more accurate baseline data. This would be the first step towards the ultimate goal of using hyperspectral remote sensing to discriminate and map the distribution of invasive species in protected areas that will aid in the management perspectives.

Conflicts of Interest: The authors declare no conflict of interest.

Appendix A

Table A1. Results of Holm–Bonferroni post hoc tests of all pairs of plant species using pair comparison plot app (significance level: * = $p < 0.05$, ** = $p < 0.01$, *** = $p < 0.001$, n.s = non-significant).

	Plant Pairs	GMI	REP	PRI	GI	LCI	SRPI	WI	NDVI	VREI	Frequency of Different Indices (%)	
1	AM JA	n.s.	***	n.s.	n.s.	n.s.	n.s.	**	n.s.	***	3	33
2	AM CV	n.s.	n.s.	n.s.	n.s.	n.s.	n.s.	n.s.	n.s.	n.s.	0	0
3	AM EC	n.s.	***	n.s.	n.s.	n.s.	n.s.	n.s.	n.s.	***	2	22
4	AM LC	n.s.	n.s.	n.s.	n.s.	n.s.	n.s.	n.s.	n.s.	n.s.	0	0
5	AM LL	n.s.	n.s.	n.s.	n.s.	n.s.	*	**	n.s.	n.s.	3	33
6	AM PH	n.s.	n.s.	n.s.	**	n.s.	**	n.s.	*	*	5	56
7	AM PJ	n.s.	**	n.s.	*	n.s.	n.s.	n.s.	n.s.	*	3	33
8	AM PP	**	***	n.s.	n.s.	**	n.s.	n.s.	n.s.	***	4	44
9	AM TS	n.s.	n.s.	n.s.	n.s.	n.s.	*	n.s.	n.s.	n.s.	1	11
10	JA CV	*	***	*	*	**	n.s.	n.s.	n.s.	***	6	67
11	JA EC	n.s.	n.s.	n.s.	*	n.s.	n.s.	*	n.s.	n.s.	2	22
12	JA LC	n.s.	*	*	**	n.s.	n.s.	**	n.s.	***	5	56
13	JA LL	*	**	n.s.	**	n.s.	*	***	n.s.	**	6	67
14	JA PH	**	***	*	***	***	**	*	**	n.s.	8	89
15	JA PJ	n.s.	n.s.	*	**	n.s.	n.s.	n.s.	n.s.	n.s.	2	22
16	JA PP	n.s.	n.s.	n.s.	n.s.	n.s.	n.s.	*	n.s.	n.s.	1	11
17	JA TS	n.s.	**	**	n.s.	*	*	*	*	**	7	78
18	CV EC	n.s.	***	*	n.s.	*	**	n.s.	n.s.	***	5	56
19	CV PP	***	***	n.s.	n.s.	***	n.s.	n.s.	*	***	5	56
20	CV TS	n.s.	*	n.s.	n.s.	n.s.	n.s.	n.s.	n.s.	n.s.	1	11
21	DV AM	n.s.	n.s.	n.s.	n.s.	n.s.	**	n.s.	n.s.	n.s.	2	22
22	DV JA	n.s.	**	*	**	n.s.	*	**	n.s.	**	6	67
23	DV CV	n.s.	*	n.s.	n.s.	n.s.	n.s.	n.s.	n.s.	n.s.	1	11
24	DV EC	n.s.	**	**	n.s.	n.s.	***	n.s.	n.s.	**	4	44
25	DV LC	n.s.	n.s.	n.s.	n.s.	n.s.	n.s.	n.s.	n.s.	n.s.	0	0
26	DV LL	n.s.	n.s.	n.s.	n.s.	n.s.	n.s.	**	n.s.	n.s.	1	11
27	DV PH	n.s.	n.s.	n.s.	n.s.	*	n.s.	n.s.	*	n.s.	2	22
28	DV PJ	n.s.	*	n.s.	n.s.	n.s.	n.s.	n.s.	n.s.	n.s.	1	11
29	DV PP	**	***	n.s.	n.s.	*	n.s.	n.s.	n.s.	***	4	44
30	DV TS	n.s.	n.s.	n.s.	n.s.	n.s.	n.s.	n.s.	n.s.	n.s.	0	0
31	LC CV	n.s.	*	n.s.	n.s.	n.s.	n.s.	n.s.	n.s.	n.s.	1	11
32	LC EC	n.s.	**	*	n.s.	n.s.	**	n.s.	n.s.	***	4	44
33	LC LL	n.s.	n.s.	n.s.	n.s.	n.s.	n.s.	***	n.s.	n.s.	1	11
34	LC PH	n.s.	n.s.	n.s.	n.s.	*	*	n.s.	*	*	4	44
35	LC PJ	n.s.	n.s.	n.s.	n.s.	n.s.	n.s.	n.s.	n.s.	*	1	11
36	LC PP	**	***	n.s.	n.s.	*	n.s.	n.s.	n.s.	***	4	44
37	LC TS	n.s.	n.s.	n.s.	n.s.	n.s.	n.s.	n.s.	n.s.	n.s.	0	0
38	LL CV	n.s.	*	n.s.	n.s.	n.s.	n.s.	***	n.s.	n.s.	2	22
39	LL EC	n.s.	**	n.s.	n.s.	n.s.	***	***	n.s.	***	4	44
40	LL PH	n.s.	n.s.	n.s.	n.s.	n.s.	n.s.	***	*	n.s.	2	22
41	LL PJ	n.s.	*	n.s.	n.s.	n.s.	n.s.	***	n.s.	n.s.	2	22
42	LL PP	***	***	n.s.	n.s.	**	n.s.	***	n.s.	***	5	56
43	LL TS	n.s.	n.s.	n.s.	n.s.	n.s.	n.s.	***	n.s.	n.s.	1	11
44	PH CV	n.s.	n.s.	n.s.	*	n.s.	n.s.	n.s.	n.s.	*	2	22
45	PH EC	**	***	**	*	**	***	n.s.	**	*	8	89
46	PH PP	***	***	n.s.	***	***	*	n.s.	***	**	7	78
47	PH TS	n.s.	n.s.	n.s.	**	n.s.	n.s.	n.s.	n.s.	n.s.	1	11
48	PJ CV	n.s.	***	n.s.	n.s.	n.s.	n.s.	n.s.	n.s.	*	2	22
49	PJ EC	n.s.	n.s.	**	n.s.	n.s.	**	n.s.	n.s.	*	3	33

Table A1. *Cont.*

	Plant Pairs	GMI	REP	PRI	GI	LCI	SRPI	WI	NDVI	VREI	Frequency of Different Indices (%)	
50	PJ PH	n.s.	**	n.s.	n.s.	*	n.s.	n.s.	n.s.	n.s.	2	22
51	PJ PP	**	**	n.s.	*	*	n.s.	n.s.	*	**	6	67
52	PJ TS	n.s.	*	n.s.	n.s.	n.s.	n.s.	n.s.	n.s.	n.s.	1	11
53	PP EC	*	n.s.	*	n.s.	n.s.	*	n.s.	n.s.	n.s.	3	33
54	TS EC	n.s.	**	**	n.s.	*	***	n.s.	n.s.	**	5	56
55	TS PP	**	***	n.s.	n.s.	**	n.s.	n.s.	*	***	5	56

References

1. Gallardo, B.; Aldridge, D.C.; González-Moreno, P.; Pergl, J.; Pizarro, M.; Pyšek, P.; Thuiller, W.; Yesson, C.; Vilà, M. Protected areas offer refuge from invasive species spreading under climate change. *Glob. Chang. Biol.* **2017**, *23*, 5331–5343. [CrossRef]
2. Cai, H.; Lu, H.; Tian, Y.; Liu, Z.; Huang, Y.; Jian, S. Effects of invasive plants on the health of forest ecosystems on small tropical coral islands. *Ecol. Indic.* **2020**, *117*, 106656. [CrossRef]
3. Pyšek, P.; Hulme, P.E.; Simberloff, D.; Bacher, S.; Blackburn, T.M.; Carlton, J.T.; Dawson, W.; Essl, F.; Foxcroft, L.C.; Genovesi, P.; et al. Scientists' warning on invasive alien species. *Biol. Rev.* **2020**, *95*, 1511–1534. [CrossRef]
4. Orr, S.P.; Rudgers, J.A.; Clay, K. Invasive plants can inhibit native tree seedlings: Testing potential allelopathic mechanisms. *Plant Ecol.* **2005**, *181*, 153–165. [CrossRef]
5. Shabbir, A.; Dhileepan, K.; O'Donnell, C.; Adkins, S.W. Complementing biological control with plant suppression: Implications for improved management of parthenium weed (*Parthenium hysterophorus* L.). *Biol. Cont.* **2013**, *64*, 270–275. [CrossRef]
6. Shabbir, A.; Ali, S.; Khan, I.A.; Belgeri, A.; Khan, N.; Adkins, S. Suppressing parthenium weed with beneficial plants in Australian grasslands. *Int. J. Pest Manag.* **2021**, *67*, 114–120. [CrossRef]
7. Tesfamichael, S.G.; Newete, S.W.; Adam, E.; Dubula, B. Field spectroradiometer and simulated multispectral bands for discriminating invasive species from morphologically similar cohabitant plants. *GIsci. Remote Sens.* **2018**, *55*, 417–436. [CrossRef]
8. Vilà, M.; Espinar, J.L.; Hejda, M.; Hulme, P.E.; Jarošík, V.; Maron, J.L.; Pergl, J.; Schaffner, U.; Sun, Y.; Pyšek, P. Ecological impacts of invasive alien plants: A meta-analysis of their effects on species, communities and ecosystems. *Ecol. Lett.* **2011**, *14*, 702–708. [CrossRef] [PubMed]
9. Pardo-Primoy, D.; Fagúndez, J. Assessment of the distribution and recent spread of the invasive grass *Cortaderia selloana* in Industrial Sites in Galicia, NW Spain. *Flora Morphol. Distrib. Funct. Ecol. Plants* **2019**, *259*, 151465. [CrossRef]
10. Carlier, J.; Davis, E.; Ruas, S.; Byrne, D.; Caffrey, J.M.; Coughlan, N.E.; Dick, J.T.A.; Lucy, F.E. Using open-source software and digital imagery to efficiently and objectively quantify cover density of an invasive alien plant species. *J. Environ. Manag.* **2020**, *266*, 110519. [CrossRef] [PubMed]
11. Caffrey, J.M.; Baars, J.R.; Barbour, J.H.; Boets, P.; Boon, P.; Davenport, K.; Dick, J.T.A.; Early, J.; Edsman, L.; Gallagher, C.; et al. Tackling invasive alien species in Europe: The top 20 issues. *Manag. Biol. Invasions* **2014**, *5*, 1–20. [CrossRef]
12. Huang, C.Y.; Asner, G.P. Applications of remote sensing to alien invasive plant studies. *Sensors* **2009**, *9*, 4869–4889. [CrossRef]
13. Martin, F.M.; Müllerová, J.; Borgniet, L.; Dommanget, F.; Breton, V.; Evette, A. Using single- and multi-date UAV and satellite imagery to accurately monitor invasive knotweed species. *Remote Sens.* **2018**, *10*, 1662. [CrossRef]
14. Jones, H.G.; Vaughan, R.A. *Remote Sensing of Vegetation: Principles, Techniques, and Applications*; Oxford University Press: Oxford, UK, 2010. ISBN 0199207798.
15. Bazzichetto, M.; Malavasi, M.; Bartak, V.; Acosta, A.T.R.; Rocchini, D.; Carranza, M.L. Plant invasion risk: A quest for invasive species distribution modelling in managing protected areas. *Ecol. Indic.* **2018**, *95*, 311–319. [CrossRef]
16. Vaz, A.S.; Alcaraz-Segura, D.; Vicente, J.R.; Honrado, J.P. The many roles of remote sensing in invasion science. *Front. Ecol. Evol.* **2019**, *7*, 370. [CrossRef]
17. Rustamov, R.B.; Hasanova, S.; Zeynalova, M.H. (Eds.) *Multi-Purposeful Application of Geospatial Data*; IntechOpen: London, UK, 2018.
18. Xie, Y.; Sha, Z.; Yu, M. Remote sensing imagery in vegetation mapping: A review. *J. Plant Ecol.* **2008**, *1*, 9–23. [CrossRef]
19. Oumar, Z. Assessing the utility of the spot 6 sensor in detecting and mapping *Lantana camara* for a community clearing project in KwaZulu-Natal, South Africa. *S. Afr. J. Geomat.* **2016**, *5*, 214. [CrossRef]
20. Wang, R.; Gamon, J.A. Remote sensing of terrestrial plant biodiversity. *Remote Sens. Environ.* **2019**, *231*, 111218. [CrossRef]
21. Ismail, R.; Mutanga, O.; Peerbhay, K. The identification and remote detection of alien invasive plants in commercial forests: An Overview. *SAJG* **2016**, *5*, 49. [CrossRef]
22. Matongera, T.N.; Mutanga, O.; Dube, T.; Sibanda, M. Detection and mapping the spatial distribution of bracken fern weeds using the Landsat 8 OLI new generation sensor. *Int. J. Appl. Earth Obs. Geoinf.* **2017**, *57*, 93–103. [CrossRef]
23. Ustin, S.L.; Gamon, J.A. Remote sensing of plant functional types. *New Phytol.* **2010**, *186*, 795–816. [CrossRef]
24. He, K.S.; Rocchini, D.; Neteler, M.; Nagendra, H. Benefits of hyperspectral remote sensing for tracking plant invasions. *Divers. Distrib.* **2011**, *17*, 381–392. [CrossRef]

25. Asner, G.P.; Martin, R.E.; Carlson, K.M.; Rascher, U.; Vitousek, P.M. Vegetation-climate interactions among native and invasive species in Hawaiian rainforest. *Ecosystems* **2006**, *9*, 1106–1117. [CrossRef]

26. Asner, G.P.; Jones, M.O.; Martin, R.E.; Knapp, D.E.; Hughes, R.F. Remote sensing of native and invasive species in Hawaiian forests. *Remote Sens. Environ.* **2008**, *112*, 1912–1926. [CrossRef]

27. Dube, T.; Shoko, C.; Sibanda, M.; Madileng, P.; Maluleke, X.G.; Mokwatedi, V.R.; Tibane, L.; Tshebesebe, T. Remote sensing of invasive *Lantana camara* (Verbenaceae) in semiarid savanna rangeland ecosystems of South Africa. *Rangel. Ecol. Manag.* **2020**, *73*, 411–419. [CrossRef]

28. Forster, M.; Schmidt, T.; Wolf, R.; Kleinschmit, B.; Fassnacht, F.E.; Cabezas, J.; Kattenborn, T. Detecting the spread of invasive species in central Chile with a Sentinel-2 time-series. In Proceedings of the 9th International Workshop on the Analysis of Multitemporal Remote Sensing Images (MultiTemp), Bruges, Belgium, 27–29 June 2017; pp. 1–4.

29. Samiappan, S.; Turnage, G.; Hathcock, L.; Casagrande, L.; Stinson, P.; Moorhead, R. Using unmanned aerial vehicles for high-resolution remote sensing to map invasive *Phragmites australis* in coastal wetlands. *Int. J. Remote Sens.* **2017**, *38*, 2199–2217. [CrossRef]

30. Eitel, J.U.H.; Long, D.S.; Gessler, P.E.; Hunt, E.R.; Brown, D.J. Sensitivity of ground-based remote sensing estimates of wheat chlorophyll content to variation in soil reflectance. *Soil Sci. Soc. Am. J.* **2009**, *73*, 1715–1723. [CrossRef]

31. Niphadkar, M.; Nagendra, H. Remote sensing of invasive plants: Incorporating functional traits into the picture. *Int. J. Remote Sens.* **2016**, *37*, 3074–3085. [CrossRef]

32. Rosso, P.H.; Ustin, S.L.; Hastings, A. Mapping marshland vegetation of San Francisco Bay, California, using hyperspectral data. *Int. J. Remote Sens.* **2005**, *26*, 5169–5191. [CrossRef]

33. Somers, B.; Asner, G.P. Hyperspectral time series analysis of native and invasive species in Hawaiian rainforests. *Remote Sens.* **2012**, *4*, 2510–2529. [CrossRef]

34. Kattenborn, T.; Lopatin, J.; Förster, M.; Braun, A.C.; Fassnacht, F.E. UAV data as alternative to field sampling to map woody invasive species based on combined Sentinel-1 and Sentinel-2 data. *Remote Sens. Environ.* **2019**, *227*, 61–73. [CrossRef]

35. Fernandes, M.R.; Aguiar, F.C.; Silva, J.M.N.; Ferreira, M.T.; Pereira, J.M.C. Spectral discrimination of giant reed (*Arundo donax* L.): A seasonal study in riparian areas. *ISPRS J. Photogramm. Remote Sens.* **2013**, *80*, 80–90. [CrossRef]

36. Cochrane, M.A. Using vegetation reflectance variability for species level classification of hyperspectral data. *Int. J. Remote Sens.* **2000**, *21*, 2075–2087. [CrossRef]

37. Vaiphasa, C.; Ongsomwang, S.; Vaiphasa, T.; Skidmore, A.K. Tropical mangrove species discrimination using hyperspectral data: A laboratory study. *Estuar. Coast. Shelf Sci.* **2005**, *65*, 371–379. [CrossRef]

38. Ullah, S.; Schlerf, M.; Skidmore, A.K.; Hecker, C. Identifying plant species using mid-wave infrared (2.5–6µm) and thermal infrared (8–14µm) emissivity spectra. *Remote Sens. Environ.* **2012**, *118*, 95–102. [CrossRef]

39. Lehmann, J.; Kuzyakov, Y.; Pan, G.; Ok, Y.S. Biochars and the plant-soil interface. *Plant Soil* **2015**, *395*, 1–5. [CrossRef]

40. Schmidt, K.S.; Skidmore, A.K. Spectral discrimination of vegetation types in a coastal wetland. *Remote Sens. Environ.* **2003**, *85*, 92–108. [CrossRef]

41. Adam, E.; Mutanga, O. Spectral discrimination of papyrus vegetation (*Cyperus papyrus* L.) in swamp wetlands using field spectrometry. *ISPRS J. Photogramm. Remote Sens.* **2009**, *64*, 612–620. [CrossRef]

42. Aneece, I.; Epstein, H. Identifying invasive plant species using field spectroscopy in the VNIR region in successional systems of north-central Virginia. *Int. J. Remote Sens.* **2017**, *38*, 100–122. [CrossRef]

43. Taylor, S.L.; Hill, R.A.; Edwards, C. Characterising invasive non-native *Rhododendron ponticum* spectra signatures with spectroradiometry in the laboratory and field: Potential for remote mapping. *ISPRS J. Photogramm. Remote Sens.* **2013**, *81*, 70–81. [CrossRef]

44. Clark, M.L.; Roberts, D.A. Species-level differences in hyperspectral metrics among tropical rainforest trees as determined by a tree-based classifier. *Remote Sens.* **2012**, *4*, 1820–1855. [CrossRef]

45. Ghiyamat, A.; Shafri, H.Z.M.; Shariff, A.R.M. Influence of tree species complexity on discrimination performance of vegetation indices. *Eur. J. Remote Sens.* **2016**, *49*, 15–37. [CrossRef]

46. Rajah, P.; Odindi, J.; Mutanga, O.; Kiala, Z. The utility of Sentinel-2 Vegetation Indices (VIs) and Sentinel-1 Synthetic Aperture Radar The utility of Sentinel-2 Vegetation Indices (VIs) and Sentinel-1 Synthetic Aperture Radar (SAR) for invasive alien species detection and mapping Launched to accelerate biodiversity conservation. *Nat. Conserv.* **2019**, *35*, 41–61. [CrossRef]

47. Cho, M.A.; Sobhan, I.; Skidmore, A.K.; De Leeuw, J. Discriminating species using hyperspectral indices at Leaf and Canopy scales. *Int. Arch. Spat. Inf. Sci.* **2008**, *37*, 369–376.

48. Große-Stoltenberg, A.; Hellmann, C.; Werner, C.; Oldeland, J.; Thiele, J. Evaluation of continuous VNIR-SWIR spectra versus narrowband hyperspectral indices to discriminate the invasive *Acacia longifolia* within a mediterranean dune ecosystem. *Remote Sens.* **2016**, *8*, 334. [CrossRef]

49. Shahzad, A.; Jamil Hasan Kazmi, S.; Shahid Shaukat, S.; Bin Farhan, S. Mapping invasive plant species in Karachi using high resolution satellite imagery: An object based image analyses approach. *Int. J. Biol. Biotech.* **2017**, *14*, 479–484.

50. Kazmi, J.H.; Haase, D.; Shahzad, A.; Shaikh, S.; Zaidi, S.M.; Qureshi, S. Mapping spatial distribution of invasive alien species through satellite remote sensing in Karachi, Pakistan: An urban ecological perspective. *Int. J. Environ. Sci. Technol.* **2021**, 1–18. [CrossRef]

51. Nawaz, T.; Hameed, M.; Ashraf, M.; Ahmad, F.; Ahmad, M.S.A.; Hussain, M.; Ahmad, I.; Younis, A.; Ahmad, K.S. Diversity and conservation status of economically important flora of the Salt Range, Pakistan. *Pak. J. Bot.* **2012**, *44*, 203–211.
52. Saad, M.; Anwar, M.; Waseem, M.; Salim, M.; Ali, Z. Distribution range and population status of Indian grey wolf (*Canis Lupus Pallipes*) and Asiatic jackal (*Canis aureus*) in Lehri Nature Park, District Jhelum, Pakistan. *J. Anim. Plant Sci.* **2015**, *25*, 433–440.
53. Dai, J.; Roberts, D.A.; Stow, D.A.; An, L.; Hall, S.J.; Yabiku, S.T.; Kyriakidis, P.C. Mapping understory invasive plant species with field and remotely sensed data in Chitwan, Nepal. *Remote Sens. Environ.* **2020**, *250*, 1–12. [CrossRef]
54. Prospere, K.; McLaren, K.; Wilson, B. Plant species discrimination in a tropical wetland using in situ hyperspectral data. *Remote Sens.* **2014**, *6*, 8494–8523. [CrossRef]
55. Mutanga, O.; Skidmore, A.K. Narrow band vegetation indices overcome the saturation problem in biomass estimation. *Int. J. Remote Sens.* **2004**, *25*, 3999–4014. [CrossRef]
56. Gitelson, A.A.; Merzlyak, M.N. Remote estimation of chlorophyll content in higher plant leaves. *Int. J. Remote Sens.* **1997**, *18*, 2691–2697. [CrossRef]
57. Penuelas, J.; Baret, F.; Filella, I. Semi-empirical indices to assess carotenoids/chlorophyll a ratio from leaf spectral reflectance. *Photosynthetica* **1995**, *31*, 221–230.
58. Smith, R.C.G.; Adams, J.; Stephens, D.J.; Hick, P.T. Forecasting wheat yield in a Mediterranean-type environment from the NOAA satellite. *Aust. J. Agric. Res.* **1995**, *46*, 113–125. [CrossRef]
59. Datt, B. Visible/near infrared reflectance and chlorophyll content in eucalyptus leaves. *Int. J. Remote Sens.* **1999**, *20*, 2741–2759. [CrossRef]
60. Merzlyak, M.N.; Gitelson, A.A.; Chivkunova, O.B.; Rakitin, V.Y. Non-destructive optical detection of pigment changes during leaf senescence and fruit ripening. *Physiol. Plant.* **1999**, *106*, 135–141. [CrossRef]
61. Sims, D.A.; Gamon, J.A. Relationships between leaf pigment content and spectral reflectance across a wide range of species, leaf structures and developmental stages. *Remote Sens. Environ.* **2002**, *81*, 337–354. [CrossRef]
62. Vogelmann, J.E.; Rock, B.N.; Moss, D.M. Red edge spectral measurements from sugar maple leaves. *Int. J. Remote Sens.* **1993**, *14*, 1563–1575. [CrossRef]
63. Ganapol, B.D.; Johnson, L.F.; Hammer, P.D.; Hlavka, C.A.; Peterson, D.L. LEAFMOD: A new within-leaf radiative transfer model. *Remote Sens. Environ.* **1998**, *63*, 182–193. [CrossRef]
64. Baranoski, G.V.G.; Rokne, J.G. A practical approach for estimating the red edge position of plant leaf reflectance. *Int. J. Remote Sens.* **2005**, *26*, 503–521. [CrossRef]
65. Pride, M.; Priscilla, M.T.; Gara, T. Dominant wetland vegetation species discrimination and quantification using in situ hyperspectral data. *Trans. R. Soc. S. Afr.* **2020**, *75*, 229–238. [CrossRef]
66. Ferreira, M.P.; Grondona, A.E.B.; Rolim, S.B.A.; Shimabukuro, Y.E. Analyzing the spectral variability of tropical tree species using hyperspectral feature selection and leaf optical modeling. *J. Appl. Remote Sens.* **2013**, *7*, 073502. [CrossRef]
67. Bao, S.; Cao, C.; Chen, W.; Yang, T.; Wu, C. Towards a subtropical forest spectral library: Spectra consistency and spectral separability. *Geocarto Int.* **2021**, *36*, 226–240. [CrossRef]
68. Schmidt, K.S.; Skidmore, A.K. Exploring spectral discrimination of grass species in African rangelands. *Int. J. Remote Sens.* **2001**, *22*, 3421–3434. [CrossRef]
69. Das, B.; Sahoo, R.N.; Biswas, A.; Pargal, S.; Krishna, G.; Verma, R.; Chinnusamy, V.; Sehgal, V.K.; Gupta, V.K. Discrimination of rice genotypes using field spectroradiometry. *Geocarto Int.* **2020**, *35*, 64–77. [CrossRef]
70. Richards, J.A.; Jia, X. *Remote Sensing Digital Image Analysis: An Introduction*; Springer: Berlin, Germany, 1999.
71. Richards, J.A. *Remote Sensing Digital Image Analysis: An Introduction*; Springer: New York, NY, USA, 1993.
72. R Core Team. R: A Language and Environment for Statistical Computing. Available online: https://www.r-project.org/ (accessed on 10 September 2021).
73. Mutanga, O.; Ismail, R.; Ahmed, F.; Kumar, L. Using insitu hyperspectral remote sensing to discriminate pest attacked pine forests in South Africa. In Proceedings of the 28th Asian Conference on Remote Sensing, Kuala Lumpur, Malaysia, 12–16 November 2007; pp. 2089–2094.
74. Shafri, H.Z.M.; Anuar, M.I.; Seman, I.A.; Noor, N.M. Spectral discrimination of healthy and ganoderma-infected oil palms from hyperspectral data. *Int. J. Remote Sens.* **2011**, *32*, 7111–7129. [CrossRef]
75. Santos, M.J.; Ustin, S.L. Spectral identification of native and non-native plant species for biodiversity assessments. In Proceedings of the International Geoscience and Remote Sensing Symposium (IGARSS), Valencia, Spain, 22–27 July 2018; pp. 3420–3423.
76. Chance, C.M.; Coops, N.C.; Plowright, A.A.; Tooke, T.R.; Christen, A.; Aven, N. Invasive shrub mapping in an urban environment from hyperspectral and LiDAR-derived attributes. *Front. Plant Sci.* **2016**, *7*, 1–19. [CrossRef]
77. Panigrahy, S.; Kumar, T.; Manjunath, K.R. Hyperspectral leaf signature as an added dimension for species discrimination: Case study of four tropical mangroves. *Wetl. Ecol. Manag.* **2012**, *20*, 101–110. [CrossRef]
78. Roberts, D.A.; Ustin, S.L.; Ogunjemiyo, S.; Greenberg, J.; Bobrowski, S.Z.; Chen, J.; Hinckley, T.M. Spectral and structural measures of northwest forest vegetation at leaf to landscape scales. *Ecosystems* **2004**, *7*, 545–562. [CrossRef]
79. Gholizadeh, A.; Mišurec, J.; Kopačková, V.; Mielke, C.; Rogass, C. Assessment of red-edge position extraction techniques: A case study for norway spruce forests using hymap and simulated sentinel-2 data. *Forests* **2016**, *7*, 226. [CrossRef]
80. Clevers, J.G.P.W.; De Jong, S.M.; Epema, G.F.; Van Der Meer, F.; Bakker, W.H.; Skidmore, A.K.; Addink, E.A. MERIS and the red-edge position. *Int. J. App. Earth Obs. Geoinf.* **2001**, *3*, 313–320. [CrossRef]

81. Otunga, C.; Odindi, J.; Mutanga, O.; Adjorlolo, C. Evaluating the potential of the red edge channel for C3 (*Festuca* spp.) grass discrimination using Sentinel-2 and Rapid Eye satellite image data. *Geocarto Int.* **2019**, *34*, 1123–1143. [CrossRef]

82. Rouse, J.W.; Hass, R.H.; Schell, J.A.; Deering, D.W. *Monitoring Vegetation Systems in the Great Plains with ERTS*; NASA Special Publication: Washington, DC, USA, 1974.

83. Tucker, C.J. Red and photographic infrared linear combinations for monitoring vegetation. *Remote Sens. Environ.* **1979**, *8*, 127–150. [CrossRef]

84. Bratsch, S.N.; Epstein, H.E.; Buchhorn, M.; Walker, D.A. Differentiating among four Arctic tundra plant communities at Ivotuk, Alaska using field spectroscopy. *Remote Sens.* **2016**, *8*, 51. [CrossRef]

85. Chen, J.M. Evaluation of vegetation indices and a modified simple ratio for boreal applications. *Can. J. Remote Sens.* **1996**, *22*, 229–242. [CrossRef]

86. Ren, S.; Chen, X.; An, S. Assessing plant senescence reflectance index-retrieved vegetation phenology and its spatiotemporal response to climate change in the Inner Mongolian Grassland. *Int. J. Biometeorol.* **2017**, *61*, 601–612. [CrossRef]

87. Thenkabail, P.S.; Mariotto, I.; Gumma, M.K.; Middleton, E.M.; Landis, D.R.; Huemmrich, K.F. Selection of hyperspectral narrowbands (hnbs) and composition of hyperspectral twoband vegetation indices (HVIS) for biophysical characterization and discrimination of crop types using field reflectance and hyperion/EO-1 data. *IEEE J. Sel. Top. Appl. Earth Obs. Remote Sens.* **2013**, *6*, 427–439. [CrossRef]

88. Jiménez, M.; Díaz-Delgado, R. Towards a standard plant species spectral library protocol for vegetation mapping: A case study in the shrubland of Doñana National Park. *ISPRS Int. J. Geo-Inf.* **2015**, *4*, 2472–2495. [CrossRef]

89. Kganyago, M.; Odindi, J.; Adjorlolo, C.; Mhangara, P. Selecting a subset of spectral bands for mapping invasive alien plants: A case of discriminating parthenium hysterophorus using field spectroscopy data. *Int. J. Remote Sens.* **2017**, *38*, 5608–5625. [CrossRef]

90. Thenkabail, P.S.; Enclona, E.A.; Ashton, M.S.; Van Der Meer, B. Accuracy assessments of hyperspectral waveband performance for vegetation analysis applications. *Remote Sens. Environ.* **2004**, *91*, 354–376. [CrossRef]

91. Thomson, E.R.; Spiegel, M.P.; Althuizen, I.H.J.; Bass, P.; Chen, S.; Chmurzynski, A.; Halbritter, A.H.; Henn, J.J.; Jónsdóttir, I.S.; Klanderud, K.; et al. Multiscale mapping of plant functional groups and plant traits in the High Arctic using field spectroscopy, UAV imagery and Sentinel-2A data. *Environ. Res. Lett.* **2021**, *16*, 55006. [CrossRef]

92. Mutanga, O.; Skidmore, A.K. Red edge shift and biochemical content in grass canopies. *ISPRS J. Photogramm. Remote Sens.* **2007**, *62*, 34–42. [CrossRef]

93. Filella, I.; Peñuelas, J. The red edge position and shape as indicators of plant chlorophyll content, biomass and hydric status. *Int. J. Remote Sens.* **1994**, *15*, 1459–1470. [CrossRef]

94. Asner, G.P.; Martin, R.E.; Suhaili, A. Bin Sources of Canopy Chemical and Spectral Diversity in Lowland Bornean Forest. *Ecosystems* **2012**, *15*, 504–517. [CrossRef]

95. Zhang, J.; Rivard, B.; Sánchez-Azofeifa, A.; Castro-Esau, K. Intra- and inter-class spectral variability of tropical tree species at La Selva, Costa Rica: Implications for species identification using HYDICE imagery. *Remote Sens. Environ.* **2006**, *105*, 129–141. [CrossRef]

96. Xiao, Y.; Zhao, W.; Zhou, D.; Gong, H. Sensitivity analysis of vegetation reflectance to biochemical and biophysical variables at leaf, canopy, and regional scales. *IEEE Trans. Geosci. Remote Sens.* **2014**, *52*, 4014–4024. [CrossRef]

97. Thenkabail, P.S.; Smith, R.B.; De Pauw, E. Evaluation of narrowband and broadband vegetation indices for determining optimal hyperspectral wavebands for agricultural crop characterization. *Photogramm. Eng. Remote Sens.* **2002**, *68*, 607–621.

98. Lewis, M. Spectral characterization of Australian arid zone plants. *Can. J. Remote Sens.* **2002**, *28*, 219–230. [CrossRef]

99. Smith, A.M.; Blackshaw, R.E. Weed: Crop Discrimination Using Remote Sensing: A Detached Leaf Experiment. *Weed Technol.* **2003**, *17*, 811–820. [CrossRef]

100. Mutanga, O.; Skidmore, A.K.; Prins, H.H.T. Predicting in situ pasture quality in the Kruger National Park, South Africa, using continuum-removed absorption features. *Remote Sens. Environ.* **2004**, *89*, 393–408. [CrossRef]

101. Richards, J.A. *Remote Sensing Digital Image Analysis: An Introduction*; Springer: Berlin/Heidelberg, Germany, 2013; Volume 9783642300, ISBN 9783642300622.

102. Dabboor, M.; Howell, S.; Shokr, M.; Yackel, J. The Jeffries–Matusita distance for the case of complex Wishart distribution as a separability criterion for fully polarimetric SAR data. *Int. J. Remote Sens.* **2014**, *35*, 6859–6873. [CrossRef]

103. Jacobsen, A.; Jacobsen, A.; Nielsen, A.; Ejmais, R.; Groom, G.B. Spectral identification of plant communities for mapping of semi-natural grasslands. *Can. J. Remote Sens.* **2000**, *26*, 370–383. [CrossRef]

104. Ma, N.; Hu, Y.F.; Zhuang, D.F.; Wang, X.S. Determination on the optimum band combination of HJ-1A hyperspectral data in the case region of dongguan based on optimum index factor and J–M distance. *Remote Sens. Technol. Appl.* **2010**, *25*, 358–365.

105. Torbick, N.; Becker, B.; Qi, J.; Lusch, D. *Characterizing Field-Level Hyperspectral Measurements for Identifying Wetland Invasive Plant Species*; Nova Science Publishers: New York, NY, USA, 2009; pp. 97–115.